

1 **Assessing the effectiveness of irrigator-driven groundwater conservation programs to**
2 **drought: a case study of the northwestern Kansas Local Enhanced Management Areas**

3

4 **Authors:** Wayne Ndlovu^{a,b*}, Sam Zipper^{a,b*}, Timothy Foster^c

5

6 **Affiliations:**

7 a. Kansas Geological Survey, University of Kansas, Lawrence KS 66047

8 b. Department of Geology, University of Kansas, Lawrence KS 66045

9 c. School of Engineering, University of Manchester, Manchester, UK

10 *Correspondence to waynedndlovu5@gmail.com and samzipper@ku.edu

11

12 **Highlights:**

- 13 ● Model calibration and bias correction improves AquaCrop performance.
14 ● Potential to lower irrigation and improve water use efficiency during drought.
15 ● Current pumping allocations make GMD-4 LEMA ineffective for conserving water.

16

17 *Manuscript submitted to Agricultural Water Management for peer review, April 2025*

18

19

20 **Abstract**

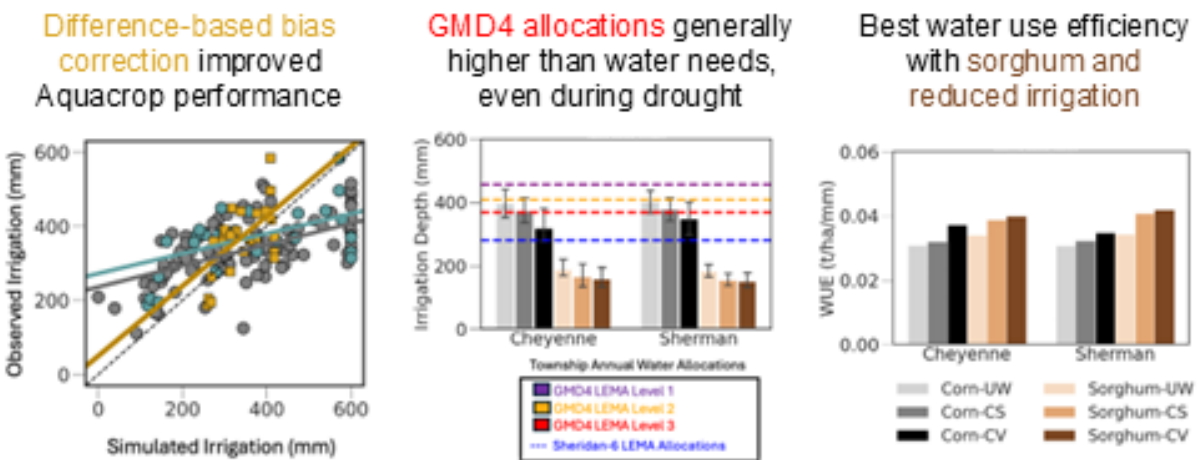
21 Groundwater pumping for irrigation has led to significant decreases in groundwater levels in
22 agricultural areas around the world, including the U.S. High Plains Aquifer. Here, we used a
23 process-based corn and sorghum crop model, AquaCrop, to assess the effectiveness of different
24 irrigation management strategies during a synthetic multi-year drought. We focused on the
25 Groundwater Management District 4 Local Enhanced Management Area (GMD-4 LEMA), a
26 regional groundwater conservation program in the northwestern Kansas portion of the High
27 Plains Aquifer. We first calibrated the AquaCrop models to observed yield and irrigation using
28 the Particle Swarm Optimization algorithm, and then applied a novel difference-based bias
29 correction method to improve performance. We found that the corn models outperformed the
30 sorghum models, likely due to limited observational sorghum data. However, both models
31 performed satisfactorily during drought periods. We then evaluated the effectiveness of the
32 groundwater conservation program, defined as the ability to reduce water use, during a synthetic
33 five-year drought under three irrigation strategies. During the synthetic drought, corn irrigation
34 requirements were double those of sorghum, but even simulated corn irrigation needs were
35 generally less than current water allocations. Model simulations also indicated that water
36 conservation strategies could reduce annual irrigation requirements without a substantial
37 reduction in crop yield through improved water use efficiency. Consistent with previous work,
38 this indicates that the current GMD-4 LEMA water allocations are ineffective for conserving
39 water.

40

41 **Keywords:**

42 AquaCrop, High Plains aquifer, groundwater management, model calibration, drought, irrigation

43 **Graphical Abstract**



44

45

46 **1. Introduction**

47 Groundwater resources across the globe are under threat due to unsustainable pumping
48 rates and changes in climate (Gorelick & Zheng, 2015). Negative impacts of groundwater level
49 declines include streamflow depletion (Lapides et al., 2023; Zipper, Brookfield, et al., 2024),
50 land subsidence (Miller et al., 2020; Teatini et al., 2006), increased groundwater extraction costs
51 (Turner et al., 2019), saltwater intrusion (Peters et al., 2022), and overall decreased water quality
52 (Dorjderem et al., 2020). As the climate continues to change and drought occurrences become
53 more frequent (Chang & Bonnette, 2016; Cook et al., 2018; Dube et al., 2022), humans, natural
54 ecosystems, and industries that rely on groundwater are faced with major challenges.
55 Groundwater depletion is particularly challenging when there is limited ability to increase
56 recharge to the aquifer, as is the case in some regions of the U.S. High Plains Aquifer (HPA).
57 The HPA underlies 450,000 km² of land covering parts of eight states (Colorado, Kansas,
58 Nebraska, South Dakota, Wyoming, New Mexico, Oklahoma and Texas; (“High Plains aquifer |
59 U.S. Geological Survey,” 2024) and supplies about a third of the water used for irrigation in the
60 US (Haacker et al., 2019). Continued depletion of the HPA poses a significant threat to food
61 production, the US economy, and the livelihood of farmers (Deines et al., 2020).

62 Potential solutions to groundwater depletion can be classified into cognitive,
63 technological, and structural fixes (Zwickle et al., 2021). Cognitive fixes aim to educate
64 irrigators on the impacts of declining aquifer levels, while technological and structural fixes
65 involve introducing more efficient irrigation techniques and changing the factors that influence
66 an irrigator’s behavior, respectively (Zeleeuw & Alfredsen, 2013). Groundwater management
67 policies are an example of structural fixes that have been implemented to address aquifer
68 depletion. Policies can be classified as either top-down or bottom-up practices. Top-down
69 policies establish a centralized government organization which formulates rules, while bottom-
70 up policies allow water users to develop their own self governance strategies (Marston et al.,
71 2022). Some have argued that top-down management practices tend to be less effective as
72 irrigators have less input on the strategies which often leads to mistrust between the irrigators
73 and governing organizations (Marston et al., 2022). Additionally, Kiparsky et al. (2017) raised
74 concerns about fairness and inefficiency of top-down management. On the other hand, bottom-up
75 governance tends to promote collaboration among water users due to interdependence since one
76 user’s actions affects the common pool resource and other’s ability to use it (Feltman, 2024).
77 However, some have argued that bottom-up management practices are primarily driven by
78 political and economic feasibility, rather than scientific knowledge, of the solution (Andresen,
79 2015), and therefore it is unknown how effective they may be.

80 Effective design of groundwater conservation programs is further challenged by climate
81 change. Groundwater management programs based on current and historical water use practices
82 may not perform as effectively in future climate conditions. Climate change-induced droughts
83 are projected to lower crop productivity in Kansas due to shortening of the crop growing season
84 and limited water availability (Araya, Kisekka, Vara Prasad, et al., 2017). However, the impacts
85 of severe drought on crop productivity in areas with pumping limits due to groundwater

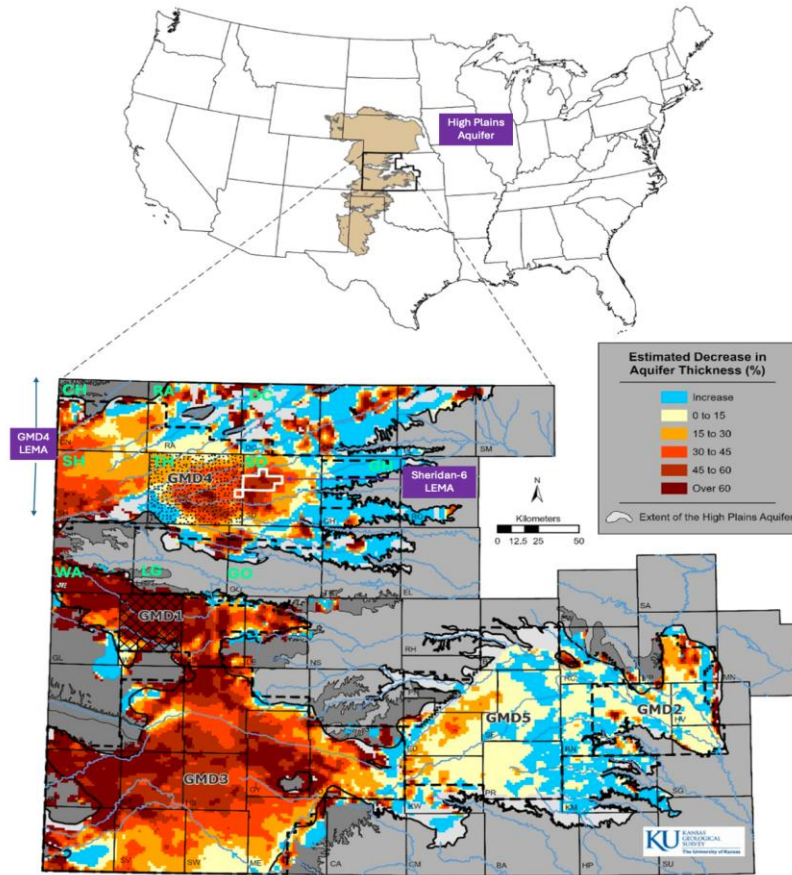
86 conservation programs are still unknown. To address this knowledge gap, crop models can be
87 used to simulate crop water productivity under varying climate scenarios. Here, we use the
88 AquaCrop crop water productivity model to simulate crop yield and water use during a five-year
89 extreme drought to assess the effectiveness of a bottom-up groundwater conservation program in
90 the Northwest Kansas Groundwater Management District 4 (GMD-4), which overlies a heavily
91 depleted portion of the HPA. To do this, this study has three objectives:

92

- 93 1. Conduct a sensitivity analysis of the AquaCrop model to determine influential parameters
94 with respect to simulated yield and water use for irrigated corn and sorghum
- 95 2. Calibrate and validate the AquaCrop model for irrigated corn and sorghum crop
96 productivity and irrigation requirements
- 97 3. Assess the effectiveness of different irrigation and crop choice strategies for groundwater
98 conservation programs under a synthetic multi-year drought.

99 2. Study area: GMD-4 LEMA

100 GMD-4 is a 12,623 km² district overlying the HPA in semi-arid northwestern Kansas and
101 includes ten counties (Fig. 1). Soils in the GMD-4 include the Ulysses-Colby Association (deep,
102 grayish-brown to dark grayish-brown silt loams), which is found in the western region, and the
103 Holdrege-Ulysses Association (deep to moderately deep, dark grayish brown silt loams and
104 moderately deep gray clays) in the eastern region (“Northwest Kansas Groundwater
105 Management District No. 4: Revised Management Plan,” 2021). Annual precipitation is
106 relatively low, averaging 17 inches in the western counties and 21 inches in the eastern counties.



107

108 **Figure 1.** Map showing the High Plains Aquifer and the estimated decreases in aquifer thickness
 109 in the Groundwater Management Districts in Kansas since the onset of widespread pumping for
 110 irrigated agriculture. The GMD-4-LEMA is located in northwest Kansas and is made up of ten
 111 counties (CH-Cheyenne, RA-Rawlins, DC-Decatur, SH-Sherman, TH-Thomas, SD-Sheridan,
 112 GH-Graham, WA-Wallace, LG-Logan, and GO-Gove). The Sheridan-6 LEMA is represented by
 113 the solid-white line. Figure modified from (Whittemore, Butler, & Wilson, 2023).

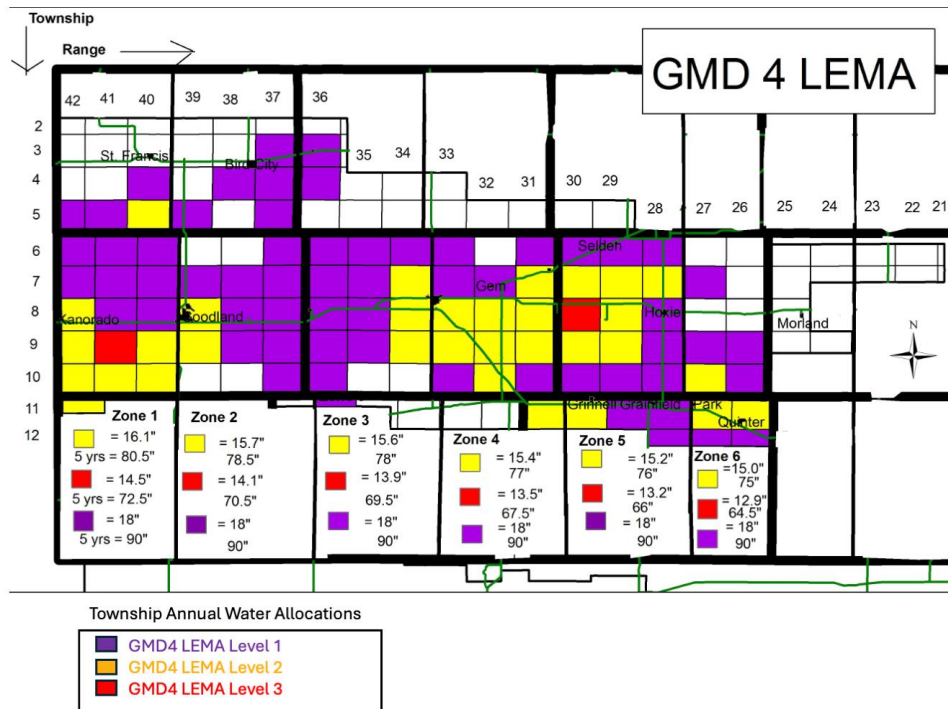
114

115 Groundwater levels in GMD-4 have declined substantially since the onset of widespread
 116 irrigation in the area (Fig. 1). In 2012, irrigators in parts of Sheridan and Thomas counties (a 255
 117 km² area within GMD-4) formed a novel groundwater conservation program called a Local
 118 Enhanced Management Area (LEMA), commonly known as the Sheridan-6 LEMA (Orduña
 119 Alegría et al., 2024). The Sheridan-6 LEMA was a bottom-up groundwater conservation
 120 program, designed by irrigators and enforced by the state, in which each water right was
 121 allocated a five-year (2013-2017) total of 1397 mm (55 inches) per irrigated ha with some
 122 variations based on water right. This translated to an overall 20% pumping reduction from
 123 historic (2002 - 2012) average use (Deines et al., 2021; Drysdale & Hendricks, 2018).
 124 Assessment of the first cycle (2013 - 2017) of the Sheridan-6 LEMA showed that it was a major
 125 success: there was an overall 67% decrease in the rate of water table decline and evidence for

126 increases in crop profitability due to (1) enhanced irrigation efficiency through the use of soil
127 moisture sensors, (2) switching from water intensive corn and soybeans to more drought tolerant
128 sorghum and wheat, and (3) prioritizing highest net profits over highest yields (Butler et al.,
129 2018; Deines et al., 2019, 2021; Orduña Alegria, 2021; Whittemore, Butler, Bohling, et al.,
130 2023). The Sheridan-6 LEMA has subsequently been renewed for additional five-year cycles for
131 2018-2022 and 2023-2027. However, the first LEMA cycle was characterized by average to
132 wetter-than-average conditions (Fig. S2) and the LEMA has not yet been stressed by a severe
133 and prolonged multi-year drought, so the resilience to potential future drought is unknown.

134 The success of the Sheridan-6 LEMA led to the creation of a district wide LEMA
135 covering the rest of GMD-4 in 2018. However, the goals and groundwater allocations within the
136 GMD-4 LEMA differed significantly from those of the Sheridan-6 LEMA. In the GMD-4
137 LEMA, groundwater decline levels reported between 2004 and 2015 were used to group areas
138 with similar annual saturated thickness decline rates into township groups. Water allocations
139 were then set based on a combination of historic water level decline rates (with lower allocations
140 for areas with higher decline rates) and position within GMD-4 (with lower allocations in the
141 eastern portion of the district where mean annual precipitation is higher). As a result, 49
142 townships were identified and five-year water allocations ranged from 2286 mm (90 inches) to
143 1638 mm (64.5 inches) (Fig. 2). For irrigators within the Sheridan-6 LEMA, the more stringent
144 limits of the Sheridan-6 LEMA superseded these township-level allocations.

145



147

148 **Figure 2.** Map showing the GMD-4 LEMA zones and water allocations. The purple boxes
 149 represents the GMD-4 LEMA Level 1 allocations (townships with a 0.5% - 1.0% average annual
 150 decline), yellow boxes the GMD-4 LEMA Level 2 allocations (townships with a 1.0% - 2.0%
 151 average annual decline), and the red boxes the GMD-4 LEMA Level 3 allocations (townships
 152 with +2.0% average annual decline). Figure modified from map prepared by Shannon Kenyon,
 153 GMD-4 (“GMD 4 LEMA,” 2024).

154

155 **3. Methods**

156 To assess the effectiveness of the GMD-4 LEMA to severe drought, we used a process-based
 157 crop model (AquaCrop) trained on historical data. In this section, we describe the AquaCrop
 158 model, the input and observational data used, and the calibration and model bias correction
 159 methods used, and the drought scenarios simulated.

160 **3.1 AquaCrop Model**

161 A number of carbon-, radiation-, and water-driven crop models have been used to
 162 simulate crop productivity using mathematical relations that link the crop, environmental, and
 163 management conditions. Common crop models used for assessing irrigation and yield response
 164 to variable climate and management conditions include AquaCrop (Steduto et al., 2009), DSSAT
 165 (Jones et al., 2003), APSIM (McCown et al., 1996), EPIC (Cavero et al., 2000), AgroIBIS
 166 (Kucharik, 2003), and ARCWHEAT (Weir et al., 1984). These types of models have been
 167 applied to address a variety of management-relevant questions in irrigated landscapes, including

168 the impacts of limiting irrigation on crop yield (Araya et al., 2016; Araya, Kisekka, Vara Prasad,
169 et al., 2017), the effects of rooting depth and planting density on crop yield (Nyakudya &
170 Stroosnijder, 2014), and the impacts of projected climate change on crop yield (Onyekwelu et al.,
171 2024; Reilly et al., 2003).

172 The AquaCrop model is a widely-used crop water productivity model developed by the
173 United Nations Food and Agriculture Organization. AquaCrop uses a soil water balance
174 approach at the daily timestep to calculate the growth and water requirements for agricultural
175 crops (Raes et al., 2009). Crop growth and irrigation requirements are determined primarily by
176 the soil water depletion in the root zone. For irrigated crops, the user can set a soil moisture
177 threshold (*smt*) to trigger irrigation. The *smt* is defined as a percentage of the Total Available soil
178 Water (*TAW*), which is the depth of plant available water in the root zone at field capacity (W_{FC})
179 after subtracting out the depth of plant available water at permanent wilting point (W_{PWP}) as
180 shown in Eq. 1:

$$181 \quad TAW = W_{FC} - W_{PWP} \quad (1)$$

182 The irrigation depth is then calculated based on the soil water depletion as described in
183 the Supplementary Material. The crop growth is also simulated daily by first estimating canopy
184 cover (*CC*) followed by the growth of above-ground crop biomass which is estimated using the
185 product of the ratio of the daily ratio of transpiration (*Tr*) to reference evapotranspiration (*ET_o*)
186 and the normalized water productivity (*WP**). From biomass (*B*), crop yield can then be
187 calculated as the product of the reference harvest index (*HIO*), *B*, and the harvest index
188 adjustment factor for stress (*fHI*) such as soil water depletion and excess heat or cold (Eq. 2):

$$189 \quad Crop\ Yield\ (Y) = fHI * B * HIO \quad (2)$$

190
191
192 In this study, we used AquaCrop-OSPy, which is the open source Python implementation
193 of AquaCrop (Foster et al., 2017; Kelly & Foster, 2021), referred to as ‘AquaCrop’ throughout
194 the manuscript for brevity. A more detailed description of AquaCrop is provided in the
195 Supplemental Material and associated references.

196 3.2 Data Sources

197
198 The required input for the AquaCrop model includes daily meteorological data
199 (precipitation, minimum temperature, maximum temperature, and reference evapotranspiration),
200 crop parameters, management parameters, and soil data (Xing et al., 2017). Since this study
201 focused on regional groundwater conservation patterns, we consolidated the field-scale level
202 input data and calculated the county level average soil and average daily meteorological
203 conditions as described below. For the 2006-2020 study period, we used a cultivated field dataset
204 (Gao et al., 2017) to extract the dominant annual crop type from the United States Department of
205 Agriculture National Agricultural Statistics Service (USDA NASS) Cropland Data Layer (CDL)
206 (“USDA National Agricultural Statistics Service Cropland Data Layer,” 2023) the Annual

207 Irrigation Maps - High Plains Aquifer (AIM-HPA) dataset as in Zipper, Kastens, et al., (2024).
208 Since our study focused on irrigated corn and sorghum, we then averaged soil type from the
209 Probabilistic Remapping of SSURGO (POLARIS; Chaney et al., 2016) dataset and daily
210 meteorological data from the Gridded Surface Meteorological (gridMET; Abatzoglou, 2013)
211 dataset. Planting dates for each year were defined based on the annual planting dates in the
212 northwestern Kansas region since field-specific planting dates were not available (“USDA -
213 National Agricultural Statistics Service - Charts and Maps - County Maps,” 2023).

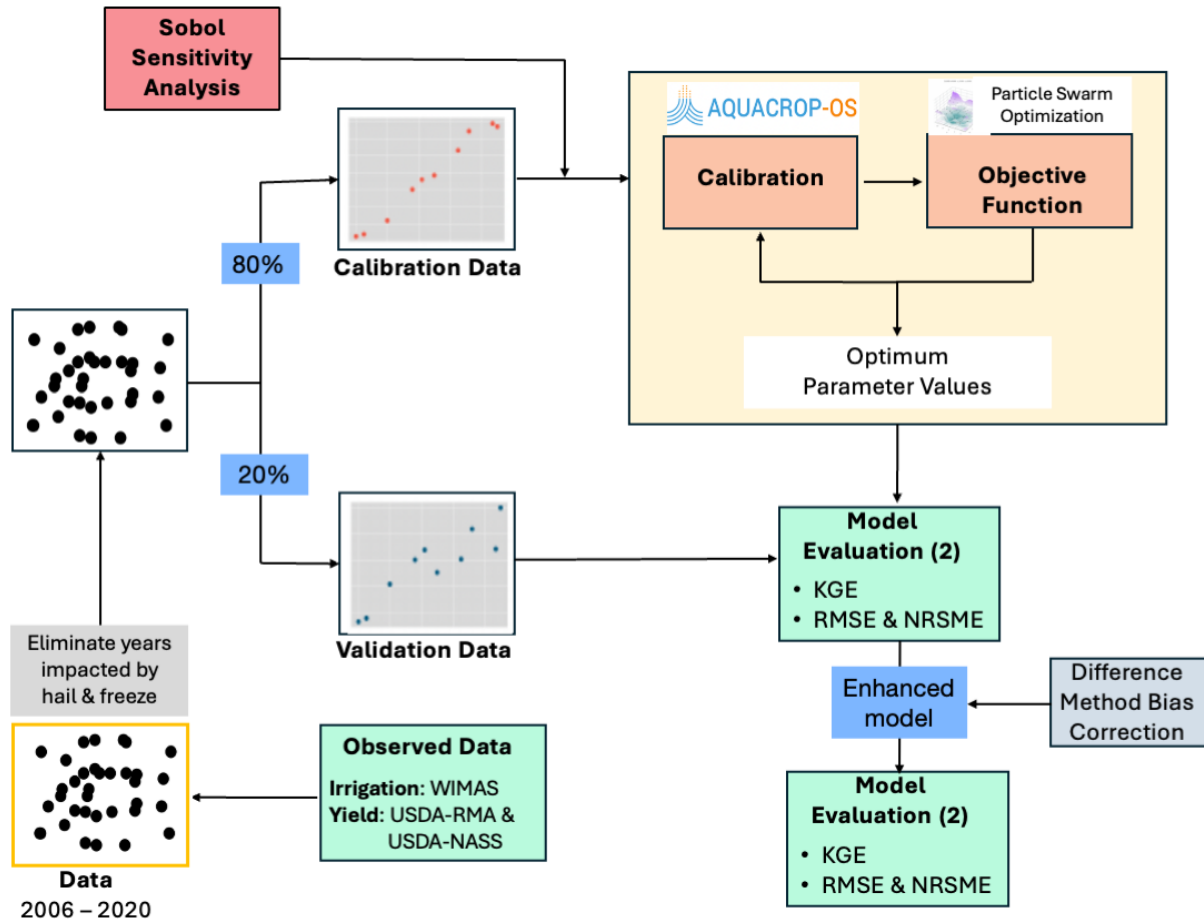
214 To calibrate and evaluate the model’s performance, we used observed irrigation and crop
215 yield data for each county. Irrigation depths in the GMD-4 region were extracted from the
216 Kansas Water Information and Management and Analysis System (WIMAS) well data
217 (“WIMAS,” 2023) a statewide pumping database that irrigators are required to submit annual
218 pumping volumes, crop types, and irrigated acreage. Following methods by Obembe et al.,
219 (2023), we first excluded wells that reported irrigation on areas <40 acres or >500 acres, and
220 those with irrigation depths outside of the 1st and 99th percentile, to eliminate outliers that may
221 be linked to misreported or misrecorded data. For each county and year, we then calculated the
222 annual median irrigation depth for corn and sorghum. We eliminated counties where the
223 specified crop (corn or sorghum) was grown less than three times over the entire study period to
224 ensure a more robust analysis.

225 We obtained annual county level yield data for the 2006 to 2020 period for the 10
226 counties in the GMD-4 area from the Kansas State - Extension Yield Correlation Tool
227 ([https://www.agmanager.info/crop-insurance/crop-insurance-papers-and-information/kansas-
228 yield-correlation-tool](https://www.agmanager.info/crop-insurance/crop-insurance-papers-and-information/kansas-yield-correlation-tool)) which uses data reported by the United States Department of Agriculture
229 Risk Management Agency (USDA-RMA), and the United States Department of Agriculture
230 National Agricultural Statistics Service (USDA-NASS; “USDA/NASS QuickStats Ad-hoc
231 Query Tool,” 2023). We compared the two yield datasets and excluded any counties or years
232 where the difference between them exceeded 10% to account for potential errors in the reported
233 data since the two data sources are aggregated in different ways. Due to multiple missing
234 observations in the USDA NASS dataset, the USDA-RMA data was used as the primary dataset.
235 For instances where there were missing observations in the USDA-RMA dataset, the USDA-
236 NASS was used to fill the gaps and complete the dataset. We eliminated the years and counties
237 where hail and freeze caused significant crop losses, since these processes are not simulated by
238 AquaCrop. To do this, we removed county-years from the dataset where losses due to hail and/or
239 freeze exceeded \$1,000,000 as reported in the loss data from the United States Department of
240 Agriculture Risk- Management Agency (USDA-RMA; “Cause of Loss | RMA,” 2023).

241 *3.3 Sensitivity Analysis, Calibration, and Bias Correction*

242 The AquaCrop model was calibrated using observed yield and irrigation depth data
243 reported between 2006 and 2020 in the ten GMD-4 counties (Fig. 1). We first used the Sobol
244 Method (Sobol, 1990) to identify influential model parameters when simulating crop yield and

245 irrigation requirements, and then used a Particle Swarm Optimization (PSO) algorithm to
 246 calibrate parameters that were identified as sensitive and applied a difference bias correction
 247 method to improve model performance (Fig. 3).
 248



249
 250 **Figure 3.** Methodology for calibrating the AquaCrop model integrating sensitivity analysis,
 251 model calibration, and bias correction.

252
 253 3.3.1 Sensitivity analysis

254 Our sensitivity analysis was intended to identify parameters with the greatest influence on
 255 simulated corn and sorghum yield and irrigation under dry, normal, and wet meteorological
 256 conditions. We used 12 scenarios which were a factorial combination of the meteorological
 257 condition (dry, normal, or wet year, defined based on the lowest, median, and highest annual
 258 precipitation during the model period), crop type (corn or sorghum), and response variable
 259 (irrigation or yield). For each sensitivity analysis scenario, the Sobol method (Sobol, 1990) was
 260 applied to crop parameters related to (1) crop development and transpiration, (2) biomass and
 261 yield, (3) water stress, and (4) management using the *SALib* Python package (Herman & Usher,

262 2017). We evaluated a total of 12 parameters for corn and 8 parameters for sorghum (Table S1).
 263 Parameter ranges used in this study were obtained from the model documentation (Raes et al.,
 264 2023) and previous studies in the surrounding regions (Araya et al., 2016; Araya, Kisekka, Lin,
 265 et al., 2017; Masasi et al., 2019). For example, the maximum daily and seasonal irrigation depths
 266 during the calibration period were 6.5 mm and 600 mm for corn, and 6.5 and 450 mm for
 267 sorghum based on field observations from Kansas State Research and Extension (Ciampitti et al.,
 268 2022, 2023) and each crop's maximum observed irrigation depths from WIMAS. For parameters
 269 included in the sensitivity analysis, we analyzed the first, second and total indices using the
 270 Sobol function from the *SALib* Python package (Herman & Usher, 2017). To distinguish
 271 between the influential and non-influential parameters, we defined a threshold: parameters with
 272 total order indices (ST) greater than 10% of the maximum ST from each scenario were defined
 273 as influential. Please refer to the Supplementary Material for more details on the sensitivity
 274 analysis methods.

275

276 3.3.2 Calibration using Particle Swarm Optimization (PSO)

277 PSO is a bio-inspired global optimization algorithm based on the social behavior of
 278 biological organisms such as a flock of birds or a school of fish (Kennedy & Eberhart, 1995;
 279 Reynolds, 1987). In PSO, each particle in the swarm moves in a multidimensional search space
 280 over a given time, which is determined by the number of iterations. Each particle in the search
 281 space represents a potential solution which optimizes the objective function (Umapathy et al.,
 282 2010). The particle swarm optimization (PSO) algorithm was used because it is easier to
 283 implement, has fewer parameters, converges faster, and requires fewer computational resources
 284 than other global optimization methods (Liu et al., 2022; Noel, 2012).

285 The user specifies the population size of the 'swarm'. For each particle within the swarm,
 286 initial parameter values are randomly generated from a uniform distribution within the user
 287 specified bounds. The PSO implementation followed methods documented in previous studies
 288 (Poli et al., 2007; Wagner et al., 2020) to estimate coefficients for parameters identified as
 289 influential by the sensitivity analysis (Table 1) that maximized model fit to observed county-
 290 resolution crop yields and irrigation depths. We used a swarm size of 100 with 500 as the
 291 maximum number of iterations. Other required PSO parameters were ω (set to 0.5 following
 292 Eberhart & Shi, 2001), c_1 and c_2 (set to 2). For c_1 and c_2 , values that are less than or equal to two
 293 are mostly used (Anandakumar & Umamaheswari, 2018). The algorithm was set to terminate
 294 when the minimum change in swarm's best position and objective value were 1×10^{-8} and 0.1,
 295 respectively, or when the maximum number of iterations was reached. We defined the weighted
 296 least square's objective function as follows:

$$297 \quad S(b) = \sum w_y [y_{tc} - y_{tc}(b)]^2 + \sum w_i [i_{tc} - i_{tc}(b)]^2 \quad (3)$$

298 where:

299 w = weight of the observation where w_y and w_i are the weights for yield and irrigation
300 depth, respectively. The weights are calculated as $1/\text{variance}$.
301 y = observed yield (t/ha)
302 $y(b)$ = simulated yield (t/ha)
303 i = observed irrigation depth (mm)
304 $i(b)$ = simulated irrigation depth (mm)
305 tc = summations done over all counties and years in the training data
306

307 **Table 1.** Influential model parameters used in the model calibration (see Supplementary Material
308 for details on parameter selection and ranges). Highlighted rows indicate parameters considered
309 only for corn and the remaining parameters were used for both corn and sorghum.
310

Parameter	Description	Units
<u>Crop Development and Transpiration</u>		
ccx	maximum fractional canopy cover size	-
rtx	maximum effective rooting depth	m
kc	crop coefficient when canopy is complete but prior to senescence	-
<u>Biomass and Yield</u>		
wp	water productivity normalized for reference ET0 and CO2	g/m2
hi	reference harvest index	-
hipsveg	coefficient describing positive impact of restricted vegetative growth during yield formation on HI	-
<u>Management</u>		
smt1	soil moisture threshold during crop emergence and canopy growth	%
smt2	soil moisture threshold during crop maximum canopy	%
smt3	soil moisture threshold during crop canopy senescence	%

311
312
313 While the focus of our scenario analysis is severe drought, we incorporated all counties
314 and years with available data into our calibration and validation to increase the data available for
315 calibration purposes, thereby reducing equifinality, and because we do not expect these
316 parameters to be different in drought years. We randomly split the observed yield and irrigation
317 data into calibration and validation using an 80:20 split. We also used multi-model analysis and
318 model selection (Barnhart et al., 2020; Hill & Tiedeman, 2005; Poeter & Hill, 2007) to (1)
319 compare alternative models and (2) quantify the uncertainty of the model calibrations. Following
320 recommendations by Hill & Tiedeman (2005), fifteen alternative models were developed through
321 a factorial combination of the (1) three initial soil water contents (*field capacity (FC)*, *saturation*

322 (*SAT*) and *wilting point (WP)*) and (2) five random model input realizations. From these, we
 323 selected the best overall model for each crop to simulate irrigation depth and crop yield, which
 324 used *FC* for initial soil water content (Fig. S1, Fig. S3, Fig. S4, Table S3, Table S4). Model
 325 performances were evaluated using the Kling-Gupta Efficient (KGE; Gupta et al., 2009), root
 326 mean squared error (RMSE), and RMSE normalized by the mean (NRMSE).

327 3.3.3 Difference method for bias correction

328 Even calibrated models have inevitable limitations due to poorly constrained parameters,
 329 processes, or model conceptualization (Saltelli et al., 2020). While these limitations are
 330 commonly addressed via bias correction in hydrological and climate models (Acharya et al.,
 331 2013; Bosompemaa et al., 2025; Fang et al., 2015; Jaiswal et al., 2022), bias correction has not
 332 been widely applied to crop models, despite the potential to improve model simulation outputs.
 333 Here, we evaluated the ability of the difference method of bias correction, which establishes a
 334 correction factor based on the difference between the observed and simulated data (Kaur & Kaur,
 335 2023), to improve crop yield and irrigation simulation performance. We selected the difference
 336 method because it produced lower errors and was more efficient in a comparison of multiple
 337 bias-correction models for climate projections (Kaur & Kaur, 2023).

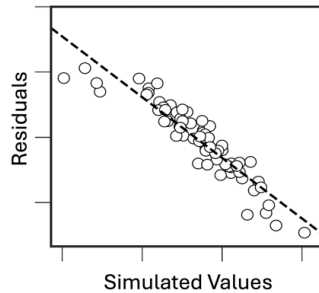
338 We implemented the difference method by establishing two additive correction factors;
 339 one for the predicted annual crop yield and another one for the irrigation. Both crop yield and
 340 irrigation were bias-corrected with a correction factor as follows:

$$341 \quad 342 \quad Y_{pred}^* = Y_{pred} + \hat{C} \quad (4)$$

343 where Y_{pred}^* and Y_{pred} denote the bias-corrected and calibrated model predictions for crop yield
 344 or irrigation. \hat{C} is the correction factor or estimated model residuals, which is calculated for all
 345 the years and counties using the linear relationship between the model predictions (Y_{pred}) and
 346 the model residuals:

$$347 \quad 348 \quad \hat{C} = mY_{pred} + b \quad (5)$$

349 where m and b are the slope and intercept of the regression line, respectively. Fig. 4 shows an
 350 example of the relationship between residuals and simulated values that is used to develop the
 351 relationship in Eq. 5. We used a linear regression since we observed a strong linear relationship
 352 between simulated values and the residual (Fig. S3 and Fig. S4), though the method would be
 353 adaptable to other functional forms.
 354



355

356 **Figure 4.** The relationship between simulated values and model residuals used to establish the
 357 correction factor for bias correction. Specific relationships for all models are shown in Fig. S3
 358 and Fig. S4.

359 *3.4 Assessing LEMA effectiveness during drought*

360 To simulate the potential effectiveness of the GMD-4 LEMA to severe drought, we used
 361 historic (2006 - 2020) meteorological data from the region to create a synthetic dataset with the
 362 five lowest growing season precipitation years during the study period (2012, 2020, 2006, 2013,
 363 and 2007; Fig. S2). For a spin-up prior to the drought, we also included five randomly selected
 364 non-drought years (Fig. S2). We then used the bias-corrected corn and sorghum models to
 365 simulate crop yield and irrigation requirements during spin-up and synthetic drought period, and
 366 assessed the impact of different water management strategies on crop productivity and irrigation
 367 requirements during the synthetic drought.

368

369 As discussed in Section 2, the LEMA operates on a five-year water allocation system and
 370 water allocations vary based on the township location and historic annual groundwater decline
 371 rates (Fig. 2). To assess the impacts of water conservation on crop yield and irrigation
 372 requirements during the drought period, we evaluated three irrigation strategies: Conservative
 373 (CV), Current Status (CS), and Unlimited Water (UW). We defined the CS scenario as the
 374 calibrated and bias-corrected models, which reflect the current irrigation practices. The target
 375 irrigation requirements under the CV and CS scenarios were based on regional irrigation
 376 practices. We then reduced the *smt* thresholds by 10% to create the CV scenario, and increased
 377 the *smt* thresholds by 10% and increased the maximum allowable seasonal irrigation to create the
 378 UW scenario (Table 2). The model defaults for maximum seasonal irrigation were used for the
 379 UW scenarios. The other model parameters remained unchanged from the calibration process.

380

381 **Table 2.** Irrigation strategies used to assess the effectiveness of the LEMA. The LEMA is
 382 represented by the CS parameter values from the model calibration. The SMT values are
 383 decreased and increased by 10% under Conservative (CV) and Unlimited Water (UW)
 384 conditions, respectively to represent variations in conservation strategies.

Parameter	Conservative (CV)	Current Status (CS)	Unlimited Water (UW)
<i>Max Irrigation (Corn)</i>	600 mm	600 mm	1000 mm
<i>Max Irrigation (Sorghum)</i>	450 mm	450 mm	1000 mm
<i>SMT</i>	Calibrated value - 10%	Calibrated value	Calibrated value + 10%

385

386 4. Results and Discussion

387 4.1 Sensitivity analysis

388 Results from the sensitivity analysis showed that there were more influential parameters
389 for crop yield compared to irrigation depth (Table 3). This is likely to be because yield
390 simulation is more complex in AquaCrop; the equations governing yield production begin with
391 the water balance calculations prior to seed germination and continue through to the estimation
392 of yield based on biomass towards the end of the plant growing cycle. For irrigation, the only
393 influential parameters were *rtx* and the *smt* parameters. The *rtx* parameter controls the rooting
394 depth, which defines the depth to which soil water can be used by the plant, and the *smt*
395 parameters all determine when and how much water is applied to the crop. For corn and sorghum
396 yield, the biomass and yield formation parameters (*wp* and *hi*) and a stress parameter (*hipsveg*,
397 which links restricted vegetative plant growth to yield changes) were influential in addition to
398 *smt* values. Additionally, we identified the canopy development and senescence parameters (*ccx*,
399 *rtx*, and *kc*) as sensitive, aligning with findings from past studies (Lu et al., 2021; Ran et al.,
400 2022). To calibrate the model for each crop, we used the influential parameters identified for
401 yield or irrigation across any of the three meteorological scenarios (Table 3, last row). Influential
402 parameters were calibrated while non-influential parameters were fixed to simplify the model
403 calibration.

404

405 **Table 3.** List of sensitive parameters for irrigation depth and crop yield under different
406 meteorological conditions. The bold final row indicates the full list of parameters used to
407 calibrate the models. Parameters are defined in Table 1.

408

Variable and Scenario	Sensitive Parameters (Corn)	Sensitive Parameters (Sorghum)
<i>Irrigation, dry year</i>	<i>rtx, smt1, smt2, smt3</i>	<i>rtx, smt1, smt2, smt3</i>
<i>Irrigation, normal year</i>	<i>rtx, smt1, smt2, smt3</i>	<i>rtx, smt1, smt2, smt3</i>
<i>Irrigation, wet year</i>	<i>rtx, smt1, smt2</i>	<i>rtx, smt1, smt2</i>
<i>Yield, dry year</i>	<i>rtx, smt1, smt2</i>	<i>rtx, hi, smt1, smt2</i>
<i>Yield, normal year</i>	<i>ccx, rtx, kc, wp, hi, smt1, smt2, smt3</i>	<i>ccx, wp, hi, smt2, smt3</i>
<i>Yield, wet year</i>	<i>ccx, rtx, kc, wp, hi, hipsveg, smt1, smt2</i>	<i>ccx, rtx, kc, wp, hi, smt1, smt2</i>
Parameters used in calibration	<i>ccx, rtx, kc, wp, hi, hipsveg, smt1, smt2, smt3</i>	<i>ccx, rtx, kc, wp, hi, smt1, smt2, smt3</i>

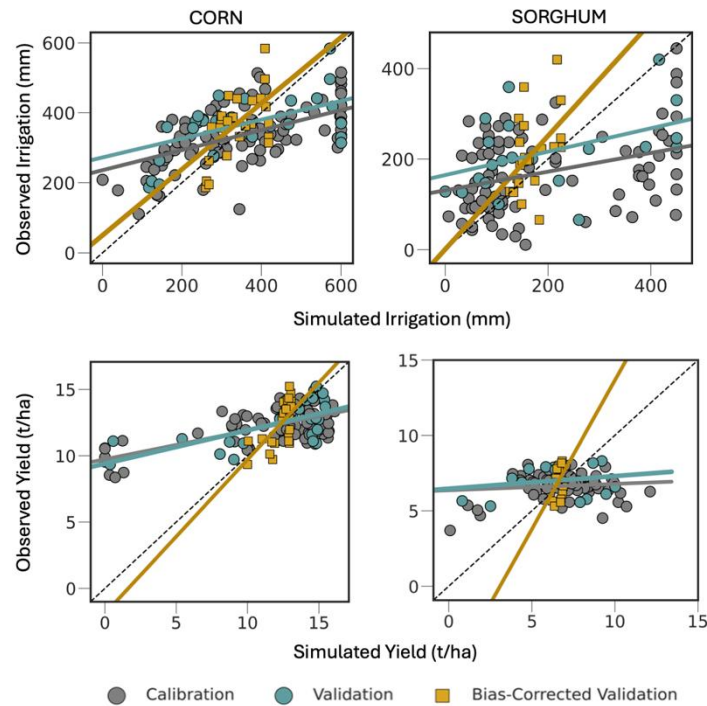
410 4.2 Model calibration and bias correction

411 4.2.1 Overall model calibration and bias correction

412 For corn, KGE for simulated irrigation depth indicated that the skill of the model was fair
413 ($-0.01 \leq KGE \leq 0.04$; Fig. 5, Table S3) and ‘acceptable’ during both the calibration and
414 validation periods, as it exceeded the performative benchmark of $KGE = -0.41$ (Knoben et al.,
415 2019). Furthermore, the corn irrigation RMSE were comparable between the calibration (127
416 mm) and validation (138 mm) stages, which indicated that the model was not subject to
417 overfitting. Due to the similar RMSE, the NRMSE was also similar in the calibration and
418 validation steps. While the models performed satisfactorily in simulating irrigation depths during
419 calibration and validation, we observed poor KGE values for corn yield during both stages (KGE
420 ≤ -0.41 ; Table S3). Despite the fair NRSME values ($NRMSE < 0.3$) for yield during these stages,
421 the RMSE values were high ($3.2 \text{ t/ha} \leq RMSE \leq 3.5 \text{ t/ha}$) and above those reported in the
422 literature, which ranged between 0.14 t/ha and 1.77 t/ha (Ahmadi et al., 2015; Heng et al., 2009;
423 Paredes et al., 2014; Sandhu & Irmak, 2019). The performance of the sorghum models were
424 generally worse for both irrigation and yield compared to the corn models (Fig. 5). For sorghum
425 irrigation, we observed ‘acceptable’ KGE values ($KGE \approx 0.07$) and high RMSE ($133 \text{ mm} \leq$
426 $RMSE \leq 143 \text{ mm}$) and NRMSE ($0.62 \leq NRMSE \leq 0.85$) values during the calibration and
427 validation stages (Fig. 5, Table S4). For sorghum yield, KGE values were poor while RMSE and
428 NRMSE were less than 2.6 t/ha and 0.38, respectively during both stages.

429 We observed a significant improvement in the model performances for both crops and
430 variables after applying the bias correction (Fig. 5). For the corn and sorghum models, there was
431 high correlation between the simulated values and the residuals prior to the bias correction
432 process ($r^2_{\text{yield}} \geq 0.66$; $r^2_{\text{irrigation}} \geq 0.86$; Fig. S3, Fig. S4), which meant that the modified
433 difference bias correction approach was effective at improving model performance without any
434 additional data beyond simulated outputs. The bias correction of the corn model resulted in fair
435 crop yield and irrigation performances with ‘medium’ KGE and ‘fair’ NRMSE values (Table
436 S3). After bias-correction, the corn models ($RMSE = 1.2 \text{ t/ha}$ (yield) and 79 mm (irrigation),
437 $NRMSE = 0.10$ (yield) and 0.22 (irrigation)) still outperformed the sorghum models ($RMSE =$
438 1.0 t/ha (yield) and 87 mm (irrigation), $NRMSE = 0.15$ (yield) and 0.41 (irrigation)), but for both
439 crops and variables the bias-corrected results provide the best match with observations compared
440 to non-bias-corrected model output. For corn yield, the RMSE and NRMSE were 1.2 t/ha and
441 0.10, respectively within the range observed in other studies (Ahmadi et al., 2015; Heng et al.,
442 2009; Paredes et al., 2014; Sandhu & Irmak, 2019). The bias correction of the sorghum model
443 improved all the fit metrics and led to crop yield RMSE (1.0 t/ha) values that were closer to the
444 0.5 t/ha - 0.7 t/ha range reported by Masasi et al., (2019) and Fazel et al., (2023). However, the
445 bias correction compromised the sorghum model's ability to accurately simulate any variations in
446 observed values. Hereafter, models without bias correction are referred to as ‘calibrated models’

447 and their simulation results as ‘calibrated’, while those with bias correction are denoted as ‘bias-
448 corrected models’ and their simulation results as ‘bias-corrected’.
449



450
451 **Figure 5.** Comparison of simulated and observed corn (left column) and sorghum (right column)
452 irrigation (top row) and yield (bottom row) during the calibration, validation, and bias-correction
453 steps.

454 4.2.2 Spatial and temporal variability in performance

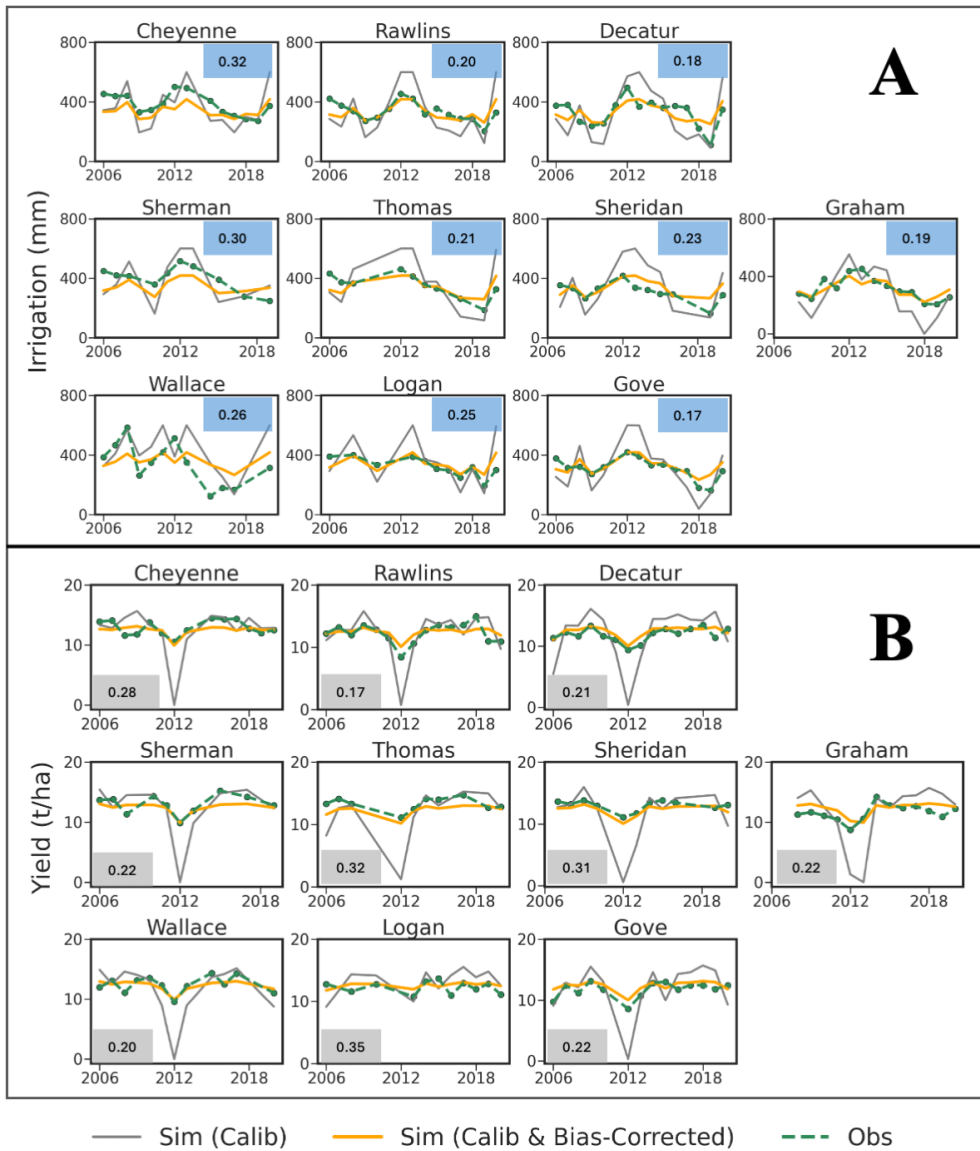
455 The corn model successfully captured the general temporal pattern observed in the
456 irrigation depths but tended to overestimate the variability of the fluctuations (Fig. 6A). For
457 example, in 2008 and 2020, as well as between 2011 and 2013, there were significant differences
458 between the observed and calibrated irrigation depths in counties located in the central and
459 eastern parts of the region (Gove, Logan, Rawlins, Sheridan and Thomas). In contrast, the bias-
460 corrected model more accurately simulated the temporal dynamics in irrigation, though it tended
461 to underestimate variability compared to observations. In the western counties (Cheyenne and
462 Sherman) with higher observed irrigation rates, the bias-corrected model underestimated
463 irrigation depths from 2006 – 2017, while it did the same in Wallace between 2006 and 2008.
464 The irrigation bias-correction was most effective for counties in the central and eastern part of
465 GMD-4, specifically Gove, Graham, and Decatur (Fig. 6A). There were fewer fluctuations in the
466 observed corn yield across all counties over the study period (Fig. 6B). During the extremely dry
467 years, such as 2011 and 2012, the calibrated model underestimated yield (<2 t/ha) and
468 overestimated irrigation requirements (Fig. 6) due to high temperature stress (above 35°C). This
469 is due to a combination of (1) a reduction in the potential harvest index due to heat stress during

470 the flowering period and (2) water stress during a high crop water demand period. Given the
471 proportional relationship between hi and yield, (Eq. 2), reductions in hi result in lower yield.
472 Moreover, temperatures above 30°C slow plant growth by limiting photosynthesis (Miller, 2018)
473 and reducing grain fill (Zhao et al., 2022). Although the calibrated model underestimated
474 irrigation applications between 2017 and 2019 in Gove and Graham counties, the simulated
475 yields were generally comparable to the observed yields suggesting difficulties in simulating
476 farmer behavior differences between years, which would not be well-captured by a crop model
477 unless it explicitly simulates time-varying decision-making processes (i.e., Lin et al., 2024), or
478 limitations related to soil hydrology that are causing incorrect relationships between irrigation,
479 soil moisture, and crop water stress (Heng et al., 2009; Sandhu & Irmak, 2019a). During these
480 years, the bias-correction model substantially improved the match between simulated and
481 observed yields.

482 The performance of the sorghum model was impacted by the limited availability of
483 observational data for irrigation and yield (Fig. 7). For example, the number of annual observed
484 irrigated sorghum fields ranged from one to seventeen. Compared to corn, there were more
485 fluctuations in the observed sorghum irrigation depths as well as lower overall irrigation rates,
486 possibly due to the smaller overall amount of sorghum being grown in the area (Zipper, Kastens,
487 et al., 2024) and therefore observed data being more subject to variability in the irrigation
488 practices of sorghum growers and the influence of potential outliers. We believe this contributed
489 to the model's difficulties in accurately capturing the dynamics of sorghum growth (Fig. 7). Our
490 analysis shows that the calibrated model tended to overestimate irrigation depths (Fig. 7A). For
491 example, in 2008 and 2011, the calibrated model failed to simulate the decreases in irrigation
492 depths in Cheyenne, Sherman and Sheridan, and instead simulated sharp increases (Fig. 7A).
493 Additionally, some of the calibrated irrigation depth peaks were out of phase with the observed
494 data such as those in Gove, Sheridan and Thomas. Although the performance of the calibrated
495 model was generally poor across most counties, its performance in Graham County was
496 exceptional and closely matched the observed data (Fig. 7A). Similar to corn yield, the drought
497 in 2012 led to low simulated crop yields and high simulated irrigation depths (Fig. 7). However,
498 due to sorghum's greater tolerance to water stress (Lamm et al., 2014), simulated sorghum yields
499 were generally more stable than those for corn.

500 Additionally, limited observational data also affected the calibration. Generally, the
501 sorghum bias correction eliminated the major peaks in the simulated data, which led to the
502 underestimation of the irrigation depths during dry years, when irrigation is higher, and
503 overestimation of irrigation depths during wet years, when irrigation is lower (Fig. 7A). Across
504 the nine counties with irrigation data, the bias correction resulted in significant improvements in
505 Thomas and Sheridan counties, beginning in 2011, when irrigation depths became consistent.
506 Although the calibrated model failed to closely match most of the observed yields, it had more
507 variability which matched some of the trends in the observed data (Fig. 7B). The bias-correction
508 yield model lowered the magnitude of the residuals for the study period, but it also eliminated
509 the model's ability to capture the fluctuations in irrigation and yield. Overall, the bias-corrected

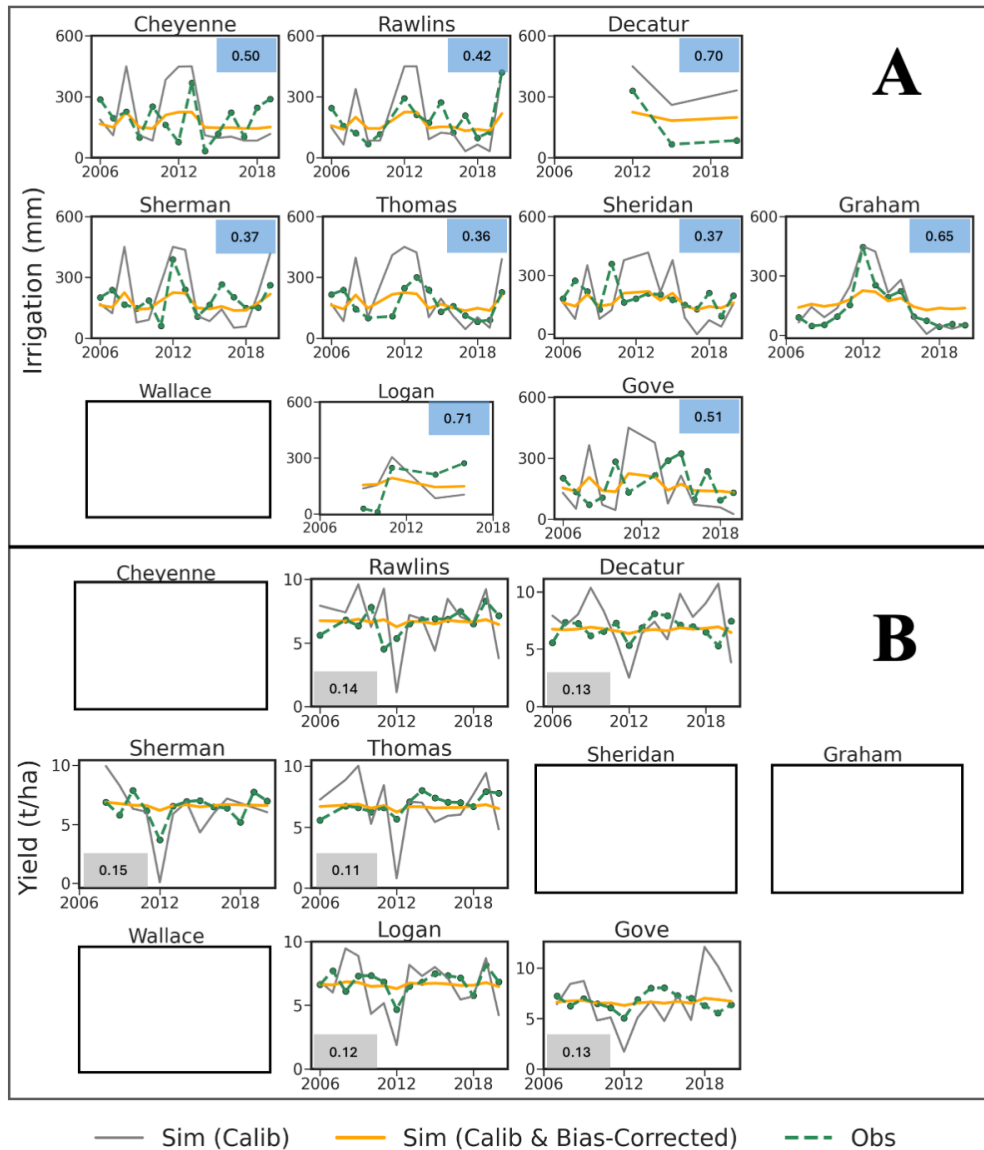
510 sorghum model outperformed the calibrated model particularly during the drier periods (2006,
 511 2007, 2012, 2013 and 2020), suggesting it is appropriate to use in our synthetic drought scenario.
 512



513

514 **Figure 6.** Comparison of observed, calibrated and bias-corrected irrigation and yield for corn
 515 over the 2006 - 2020 period for each county in the study domain. The blue and gray boxes show
 516 the bias-corrected NRSME values for irrigation and crop yield, respectively. The panels are
 517 arranged based on the location of the counties (Fig. 1).

518



519

520 **Figure 7.** Comparison of observed, calibrated and bias-corrected irrigation and yield for
 521 sorghum over the 2006 - 2020 period for each county in the study domain. The blue and gray
 522 boxes show the bias-corrected NRSME values for irrigation and crop yield, respectively. The
 523 panels are arranged based on the location of the counties (Fig. 1).

524 4.2.3 Utility of bias-corrected models

525 Since the focus of our modeling exercise was assessing the potential effectiveness of the
 526 GMD-4 LEMA during severe drought conditions, we specifically examined the bias-corrected
 527 models' capabilities during dry periods. As discussed in previous sections, the bias-corrected
 528 corn model performed satisfactorily throughout the study period (Fig. 6). During extreme
 529 drought periods such as 2012 and 2013, the bias-corrected model accurately simulated the decrease
 530 in crop yield. For most counties in the central and eastern parts of the GMD-4 region, the

531 increase in irrigation depths was correctly simulated. However, for counties in the west
532 (Cheyenne, Sherman, and Wallace), which had slightly higher observed irrigation depths, the
533 bias-corrected model underestimated the irrigation requirements by about 50 mm. On the other
534 hand, improvements in the bias-corrected sorghum model were not as strong, as discussed in
535 Section 4.2.2, which led to consistently biased corrected values (Fig. 7). While alternate bias
536 correction approaches, such as a non-linear or segmented difference-based bias correction may
537 have provided a better fit, the relationships between residuals and simulated sorghum yield were
538 highly linear except at the very highest residuals, where they flattened off (Fig. S4). This
539 suggests that the incorporation of additional variables for model calibration that can address
540 these extreme years, or application of alternate bias-correction functional forms, may improve
541 performance. For sorghum yield, the bias-corrected model simulated values of about 6 t/ha while
542 the observed yield ranged between 3 t/ha and 8 t/ha. In countries that experienced a major
543 increase in pumping rates during the 2012 drought (Sherman and Graham), the model severely
544 underestimated the irrigation requirements by close to 200 mm. However, in 2006 and 2007
545 which had low precipitation, the differences between the observed and bias-corrected crop yield
546 and irrigation depths were within acceptable ranges and generally less than 1.5 t/ha and 50 mm,
547 respectively. Since the bias-corrected corn model successfully captures most spatial and temporal
548 patterns, we conclude that it can be effectively used in studies investigating regional agricultural
549 water management objectives, including those focused on crop-water productivity during
550 extreme drought.

551 Our analysis accounted for various sources of model uncertainty, such as the uncertainty
552 due to initial soil moisture conditions, input parameters and the calibration optimization
553 algorithm used. However, disentangling the proportions of uncertainties from each source
554 remains challenging for crop models, particularly since they are primarily calibrated and
555 assessed relative to year-end values (yield and irrigation). Since many different factors interact to
556 determine these year-end values, crop models are subject to model equifinality, meaning that
557 multiple model parameterizations can provide similar performance (Lamsal et al., 2018).
558 Therefore, it is therefore difficult to determine precisely which specific uncertainties the bias
559 correction method addresses. Although several bias correction methods have been proposed in
560 previous literature (Section 3.3.3), a major limitation is that they typically require large datasets
561 and daily-scale data. Given that our study is based on limited annual data, these methods were
562 not feasible for our analysis. Overall, however, our results suggest that bias-correction can be a
563 potentially valuable tool to improve the ability of models to simulate observed irrigation and
564 crop yield dynamics.

565

566 *4.3 Effectiveness of different water management strategies during severe drought*

567 4.3.1 Variation in yield, irrigation, and water use efficiency

568

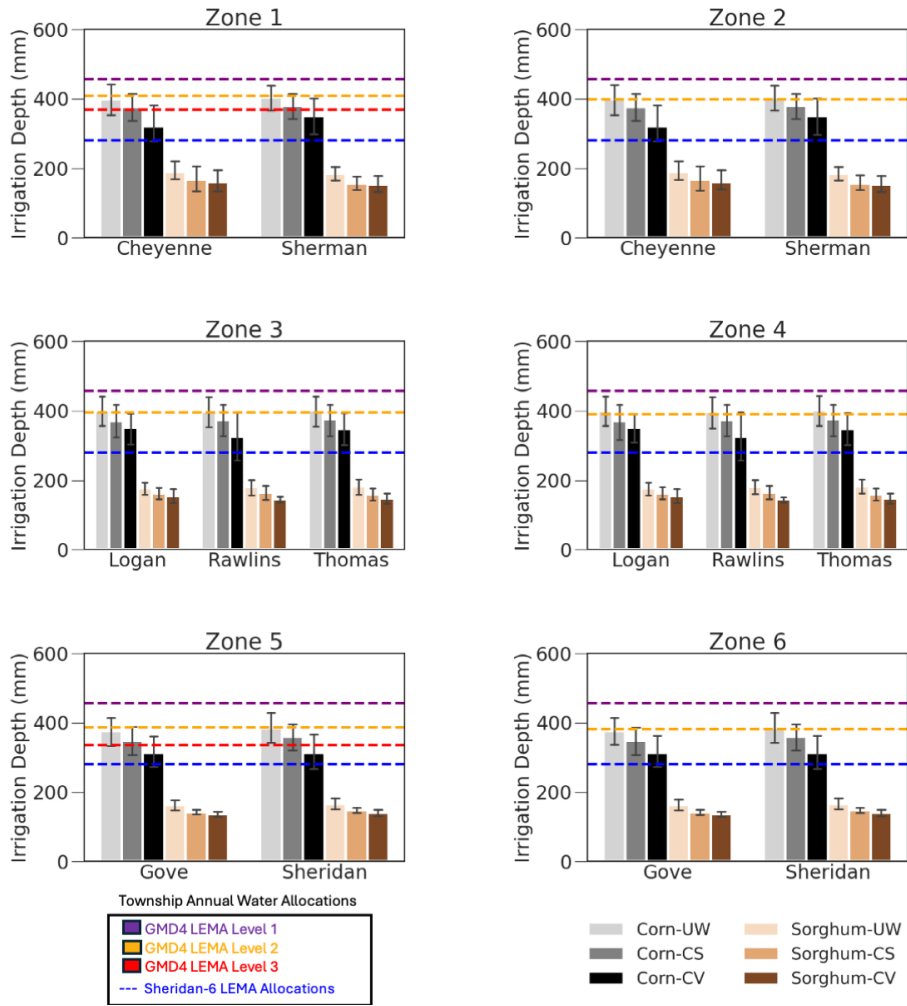
569 We evaluated the effectiveness of different irrigation management strategies (UW, CS,
570 and CV; Table 2) by comparing irrigation (Fig. 8), yield (Fig. 9), and water use efficiency (Fig.
571 10) averaged over our simulated synthetic drought scenario using the bias-corrected models for
572 the counties in the GMD-4 LEMA. We compared simulated irrigation to the average annual
573 GMD-4 and Sheridan-6 LEMA allocations to assess how each management strategy compared to
574 authorized water withdrawals. In our study, irrigation begins earlier in the UW scenario due to
575 soil moisture thresholds (SMTs) for triggering irrigation being 10% higher than in the CS
576 scenario, while it is delayed in the CV scenario due to SMT values being 10% lower than in the
577 CS scenario. As a result, irrigation is highest during the UW scenario and lowest during the CV
578 scenario. We observed relatively minor differences in the corn irrigation depths between the
579 three scenarios, with average differences between UW and CV scenarios of ~70 mm. The
580 differences among years was greatest during the driest years and caused by variation in the
581 timing and depth of irrigation application events, which was ultimately driven by the root zone
582 water balance's role in triggering irrigation (Ndlovu, 2024). For sorghum, irrigation depths
583 during the CS and CV scenarios showed little variation. The GMD-4 LEMA water allocations
584 tended to be greater than the irrigation requirements for both corn and sorghum in most zones
585 and irrigation management scenarios. Only townships in Zone 1 and 5 exceeded the Level 3
586 allocations under the corn UW scenario. However, after accounting for the model uncertainty,
587 corn irrigation under CS and UW scenarios exceeded the GMD-4 LEMA Level 2 allocation
588 limits in several zones. Corn cultivation under the three scenarios resulted in irrigation
589 application depths that were higher than the Sheridan-6 LEMA allocations in all zones.
590 Sorghum, on the other hand, required substantially less water than corn did for each scenario. As
591 a result, under sorghum cultivation none of the water allocation thresholds were exceeded.

592 Although there were differences in the corn irrigation application rates across the three
593 scenarios, their impact on crop yield was relatively small. Within a given county and
594 management zone, the crop yield differences for both corn and sorghum were less than 1.0 t/ha
595 (Fig. 9). Comparing across all six zones, for a given irrigation strategy, the simulated crop yields
596 were similar (10 t/ha – 13 t/ha range) across counties. While some of the similarity may be
597 linked to the bias correction process, in particular for sorghum (Fig. 7), the bias-corrected crop
598 models were generally able to simulate yield reductions during drought (Fig. 5, Fig. 6),
599 suggesting that the simulated yield dynamics are reasonable. However, dynamics that may occur
600 during a severe multi-year drought but were not reflected in crop yield data during our
601 calibration and validation period may not be captured here. In general, sorghum yield was
602 approximately half of corn yield, reflecting the lower overall yield potential of this crop. The
603 maximum corn yield was 13 t/ha while the maximum sorghum yield was 7 t/ha.

604 Crop water use efficiency (defined here as simulated yield per mm of simulated
605 irrigation) generally showed consistent patterns between crop type and irrigation management

606 scenarios (Fig. 10). Among crops, water use efficiency was higher for sorghum than for corn.
607 Comparing irrigation scenarios for a given crop, the greatest water use efficiency generally
608 occurred in the CV scenario. In the easternmost portion of the domain (Zones 5 and 6), the water
609 use efficiency for UW sorghum tended to still be greater than for CV corn, indicating the
610 dominant control of crop type over water use efficiency variation. In the western counties, such
611 as Zones 1-3, CV corn tended to have a greater water use efficiency than UW sorghum, but
612 lower than CS sorghum.
613

614



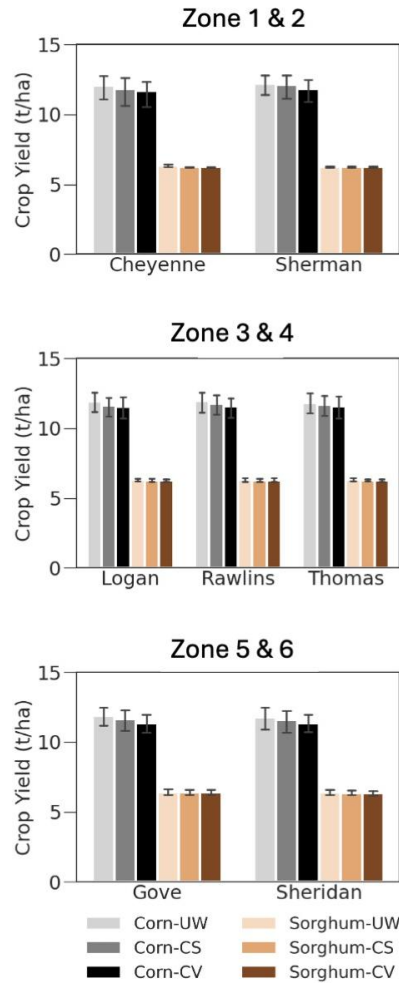
615

616

617 **Figure 8.** Predicted annual irrigation depths for corn and sorghum during synthetic drought
 618 simulation under UW, CS, and CV irrigation scenarios. The horizontal lines represent the GMD-
 619 4 LEMA allocations (Level 1 to 3) in the six zones within the GMD-4 LEMA shown in Figure 2.
 620 The blue line represents the Sheridan-6 LEMA annual allocation based on the 55 inches/5-year
 621 LEMA cycle allocation. Error bars represent the irrigation RMSE values from the bias-corrected
 622 models.

623

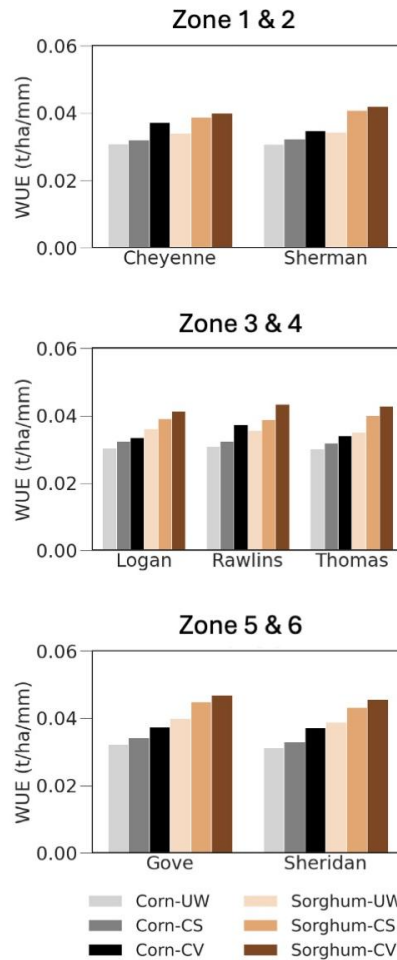
624



625

626 **Figure 9.** Predicted annual crop yield for corn and sorghum during synthetic drought simulation
 627 under UW, CS, and CV irrigation scenarios. Error bars represent the crop yield RMSE values
 628 from the bias-corrected models.

629



630

631 **Figure 10.** Predicted annual crop yield water use efficiency (WUE) for corn and sorghum during
 632 synthetic drought simulation under UW, CS, and CV irrigation scenarios.

633 4.3.2 Assessment of effectiveness

634 Comparing the simulated annual irrigation demands for corn and sorghum under CV, CS
 635 and UW scenarios to the annual GMD-4 LEMA pumping limits shows that this LEMA is
 636 ineffective, meaning that the limits would not promote reductions in water use because they are
 637 generally higher than existing crop requirements (Fig. 8). In most townships and zones, the
 638 GMD-4 LEMA can effectively support corn irrigation, which requires approximately 400 mm on
 639 average, under all three scenarios, without exceeding the GMD-4 LEMA Levels 1 to 3 pumping
 640 limits (Fig. 8). However, these corn irrigation requirements exceeded the lower average annual
 641 allocations of the Sheridan-6 LEMA (279.4 mm; 11 inches), which has effectively reduced water
 642 use (Orduna Alegria et al., 2024). These findings suggest that corn cultivation under the current
 643 GMD-4 LEMA allocations would be ineffective at conserving groundwater during prolonged
 644 droughts. This aligns with a previous assessment of the effectiveness of GMD-4 and Sheridan-6
 645 LEMA conservation practices, which showed that the Sheridan-6 LEMA was more effective at

646 reducing water use than the GMD-4 LEMA (Whittemore et al., 2023). Their study shows that the
647 first GMD-4 LEMA achieved very little water conservation while the two Sheridan-6 LEMA
648 cycles led to a 27.4% reduction in total irrigation groundwater use decrease in water table decline
649 rates from 0.43 m/year (1.4 ft/year) during the pre-LEMA to 0.18 m/year (0.6 ft/year) during the
650 LEMA (Whittemore et al., 2023). In contrast, the GMD-4 LEMA water allocations, which were
651 generally higher than the average irrigation water use during the pre-LEMA period, have only
652 affected a few irrigators with high irrigation rates due to the LEMA restrictions (Whittemore et
653 al., 2023).

654 Our study also provides evidence that switching to sorghum cultivation offers significant
655 benefits for overall groundwater conservation. During droughts, sorghum utilizes about half of
656 the GMD-4 LEMA Level 2 allocations (~180 mm) under all scenarios compared to corn which
657 requires ~90% of the allocations. Furthermore, sorghum cultivation requires irrigation
658 application rates that are within the Sheridan-6 LEMA allocations, making it a sustainable option
659 for water resource management in the region. While yield is also lower for sorghum compared to
660 corn, it typically has a greater overall water use efficiency in the region (Fig. 10). However, we
661 acknowledge that apart from crop water use, farmers in the region also select crops based on
662 economic returns, available government programs including crop insurance, crop adaptability in
663 the area and overall crop production (Hu & Beattie, 2019; Klocke et al., 2012; Zipper, Ifft, et al.,
664 2024). Based on an irrigator's priority, preference may be given to corn which is used as feed
665 grain for the beef and dairy industry and also for ethanol production (Bhattarai et al., 2020).

666 We also found that both crops had relatively little yield sensitivity to the three irrigation
667 application rates (CV, CS, and UW) that we tested (Fig. 9). This may be due to one of several
668 factors, including the relatively small (10%) changes in *smt* values between irrigation strategies,
669 issues with model calibration, or dampened sorghum yield variability caused by bias correction
670 (see Section 4.2). However, other studies have also shown that sorghum is both more water stress
671 tolerant and less responsive to irrigation compared to corn (Lamm et al., 2014). In one study,
672 Klocke et al., (2012) found total irrigation depths of 25 mm produced 91% of yields from the
673 200 mm irrigation treatment. (Eck & Musick, 1979) also indicated that sorghum yield was not
674 affected by 13 to 15 days of water stress; however, yield reductions of about 27% and 50% were
675 observed after 27 to 28 and 35 to 42 days of stress, respectively. We found that reducing corn
676 irrigation by up to 70 mm between the UW and CV scenarios led to crop yield differences that
677 were less than 1.0 t/ha (Fig. 9). A field study done in Kansas showed that limiting irrigation by
678 about 60 mm - 70 mm led to average yield that was 95% of the full irrigation treatment (Klocke
679 et al., 2012). Similarly, in Texas, 75% (413 mm) and 100% (550) irrigation treatments resulted in
680 similar end of season crop yield for one of the irrigation sprinkler methods (Schneider & Howell,
681 1998). Moreover, the overall yield difference between the 75% and 100% irrigation treatments
682 across all four sprinkler methods was only 1.5 t/ha (Schneider & Howell, 1998). Therefore, our
683 results highlight the potential to improve water use efficiency by reducing crop irrigation rates
684 without significant yield losses, even during prolonged droughts.

685 **5. Conclusions**

686 The goals of this study were to calibrate the corn and sorghum AquaCrop models for GMD-4
687 LEMA using sensitivity analysis, the PSO algorithm, and a novel bias-correction approach; and
688 use the calibrated models to assess the effectiveness of different irrigation management strategies
689 relative to local LEMA water allocation limits during a synthetic five-year drought. From this
690 analysis, the key findings were:

- 691 1. In GMD-4, AquaCrop was better at simulating corn irrigation and yield compared to
692 sorghum. The worse sorghum performance is likely due to limited observational data,
693 leading to challenges in model calibration. However, both models had some limitations
694 in capturing the spatial pattern of the observed data, particularly the higher irrigation
695 requirements in the western portion of GMD-4.
- 696 2. The incorporation of a residual-based difference method for bias correction substantially
697 improved irrigation and yield simulation performance for both crops. Overall, the
698 difference method bias correction worked better for corn models, which had fewer
699 variations in observed data, than for sorghum models. Performance improvements were
700 particularly notable during the extremely dry periods, such as the 2012 drought.
- 701 3. Under our synthetic drought simulations, all three water management scenarios were able
702 to maintain high crop yield. Simulated irrigation depths during the synthetic drought were
703 generally below the GMD-4 LEMA water allocations, suggesting that the high water
704 allocations may be ineffective for conserving water. However, the corn irrigation
705 requirements exceeded the Sheridan-6 LEMA allocations, which have been effective in
706 promoting groundwater conservation in the region.
- 707 4. During the multi-year severe drought scenario, there was a relatively small impact of
708 decreasing irrigation application on crop yield for both crops. This highlights the
709 potential to reduce crop irrigation rates without significant yield losses during extended
710 droughts through improved water use efficiency.

711 **Acknowledgments**

712 This work was supported by National Aeronautics and Space Administration (NASA) [grant
713 number 80NSSC22K1276] and National Science Foundation (NSF) [grant number RISE-
714 2108196]. TF was also supported by Innovate UK [award number 10044695], as part of the UK
715 Research and Innovation and European Commission funded project ‘TRANSCEND:
716 Transformational and robust adaptation to water scarcity and climate change under deep
717 uncertainty’. We appreciate useful feedback and suggestions from Jim Butler, Rick Devlin, Mary
718 Hill, Malena Orduna Alegria, Greg Tucker, and Brownie Wilson. We acknowledge computing
719 time on the CU-CSDMS High-Performance Computing Cluster and appreciate computing
720 support from Mark Piper. This manuscript is adapted from Ndlovu’s M.S. thesis, available at
721 [https://www.proquest.com/dissertations-theses/assessing-effectiveness-resilience-](https://www.proquest.com/dissertations-theses/assessing-effectiveness-resilience-groundwater/docview/3160666385/se-2)
722 [groundwater/docview/3160666385/se-2](https://www.proquest.com/dissertations-theses/assessing-effectiveness-resilience-groundwater/docview/3160666385/se-2)

723 **Data Statement**

724 Data and code from this study will be placed into the HydroShare repository at the time of
725 manuscript acceptance and a link with DOI will be included in the final study.

726 **Author Contributions**

727 Ndlovu: Conceptualization, Data curation, Formal Analysis, Investigation, Methodology,
728 Software, Validation, Visualization, Writing – original draft, Writing – review & editing
729

730 Zipper: Conceptualization, Funding acquisition, Methodology, Project administration,
731 Resources, Supervision, Writing – review & editing
732

733 Foster: Funding acquisition, Methodology, Software, Writing – review & editing

734 **References**

735 Abatzoglou J. T. (2013). gridMET. Retrieved December 7, 2022, from
736 <https://www.climatologylab.org/gridmet.html>

737 Acharya, N., Chattopadhyay, S., Mohanty, U. C., Dash, S. K., & Sahoo, L. N. (2013). On the
738 bias correction of general circulation model output for Indian summer monsoon.
739 *Meteorological Applications*, 20(3), 349–356. <https://doi.org/10.1002/met.1294>

740 Ahmadi, S. H., Mosallaeepour, E., Kamgar-Haghighi, A. A., & Sepaskhah, A. R. (2015).
741 Modeling Maize Yield and Soil Water Content with AquaCrop Under Full and Deficit
742 Irrigation Managements. *Water Resources Management*, 29(8), 2837–2853.
743 <https://doi.org/10.1007/s11269-015-0973-3>

744 Anandakumar, H., & Umamaheswari, K. (2018). A bio-inspired swarm intelligence technique
745 for social aware cognitive radio handovers. *Computers & Electrical Engineering*, 71,
746 925–937. <https://doi.org/10.1016/j.compeleceng.2017.09.016>

747 Andresen, S. (2015). International Climate Negotiations: Top-down, Bottom-up or a
748 Combination of Both? *The International Spectator*, 50(1), 15–30.
749 <https://doi.org/10.1080/03932729.2014.997992>

750 Araya, A., Kisekka, I., & Holman, J. (2016). Evaluating deficit irrigation management strategies
751 for grain sorghum using AquaCrop. *Irrigation Science*, 34(6), 465–481.
752 <https://doi.org/10.1007/s00271-016-0515-7>

753 Araya, A., Kisekka, I., Vara Prasad, P. V., & Gowda, P. H. (2017). Evaluating Optimum Limited
754 Irrigation Management Strategies for Corn Production in the Ogallala Aquifer Region.
755 *Journal of Irrigation and Drainage Engineering*, 143(10), 04017041.
756 [https://doi.org/10.1061/\(ASCE\)IR.1943-4774.0001228](https://doi.org/10.1061/(ASCE)IR.1943-4774.0001228)

757 Araya, A., Kisekka, I., Lin, X., Vara Prasad, P. V., Gowda, P. H., Rice, C., & Andales, A.
758 (2017). Evaluating the impact of future climate change on irrigated maize production in
759 Kansas. *Climate Risk Management*, 17, 139–154.

760 <https://doi.org/10.1016/j.crm.2017.08.001>

761 Bhattarai, B., Singh, S., West, C. P., Ritchie, G. L., & Trostle, C. L. (2020). Water Depletion
762 Pattern and Water Use Efficiency of Forage Sorghum, Pearl millet, and Corn Under
763 Water Limiting Condition. *Agricultural Water Management*, 238, 106206.
764 <https://doi.org/10.1016/j.agwat.2020.106206>

765 Bosompemaa, P., Brookfield, A., Zipper, S., & Hill, M. C. (2025). Using national hydrologic
766 models to obtain regional climate change impacts on streamflow basins with
767 unrepresented processes. *Environmental Modelling & Software*, 183, 106234.
768 <https://doi.org/10.1016/j.envsoft.2024.106234>

769 Butler, J. J., Whittemore, D. O., Wilson, B. B., & Bohling, G. C. (2018). Sustainability of
770 aquifers supporting irrigated agriculture: a case study of the High Plains aquifer in
771 Kansas. *Water International*, 43(6), 815–828.
772 <https://doi.org/10.1080/02508060.2018.1515566>

773 Cavero, J., Farre, I., Debaeke, P., & Faci, J. M. (2000). Simulation of Maize Yield under Water
774 Stress with the EPICphase and CROPWAT Models. *Agronomy Journal*, 92(4), 679–690.
775 <https://doi.org/10.2134/agronj2000.924679x>

776 Chaney, N. W., Wood, E. F., McBratney, A. B., Hempel, J. W., Nauman, T. W., Brungard, C.
777 W., & Odgers, N. P. (2016). POLARIS: A 30-meter probabilistic soil series map of the
778 contiguous United States. *Geoderma*, 274, 54–67.
779 <https://doi.org/10.1016/j.geoderma.2016.03.025>

780 Chang, H., & Bonnette, M. R. (2016). Climate change and water-related ecosystem services:
781 impacts of drought in california, usa. *Ecosystem Health and Sustainability*, 2(12),
782 e01254. <https://doi.org/10.1002/ehs2.1254>

783 Ciampitti, I., Carcedo, A. J. P., Diaz, D. R., Onfre, R. B., Lancaster, S., Whitworth, R. J., &
784 Aguilar, J. (2022). *Kansas Sorghum Management* (No. MF3046). Kansas State
785 University.

786 Ciampitti, I., Correndo, A., Lancaster, S., Diaz, D. R., Aguilar, J., Sharda, A., et al. (2023).
787 *Kansas Corn Management* (No. MF3208). Kansas State University.

788 Cook, B. I., Mankin, J. S., & Anchukaitis, K. J. (2018). Climate Change and Drought: From Past
789 to Future. *Current Climate Change Reports*, 4(2), 164–179.
790 <https://doi.org/10.1007/s40641-018-0093-2>

791 Deines, J. M., Kendall, A. D., Butler, J. J., & Hyndman, D. W. (2019). Quantifying irrigation
792 adaptation strategies in response to stakeholder-driven groundwater management in the
793 US High Plains Aquifer. *Environmental Research Letters*, 14(4), 044014.
794 <https://doi.org/10.1088/1748-9326/aafe39>

795 Deines, J. M., Schipanski, M. E., Golden, B., Zipper, S. C., Nozari, S., Rottler, C., et al. (2020).
796 Transitions from irrigated to dryland agriculture in the Ogallala Aquifer: Land use
797 suitability and regional economic impacts. *Agricultural Water Management*, 233,
798 106061. <https://doi.org/10.1016/j.agwat.2020.106061>

799 Deines, J. M., Kendall, A. D., Butler, J. J., Basso, B., & Hyndman, D. W. (2021). Combining

800 Remote Sensing and Crop Models to Assess the Sustainability of Stakeholder-Driven
801 Groundwater Management in the US High Plains Aquifer. *Water Resources Research*,
802 57(3), e2020WR027756. <https://doi.org/10.1029/2020WR027756>

803 Dorjderem, B., Torres-Martínez, J. A., & Mahlknecht, J. (2020). Intensive long-term pumping in
804 the Principal-Lagunera Region aquifer (Mexico) causing heavy impact on groundwater
805 quality. *Energy Reports*, 6, 862–867. <https://doi.org/10.1016/j.egy.2019.11.020>

806 Drysdale, K. M., & Hendricks, N. P. (2018). Adaptation to an irrigation water restriction
807 imposed through local governance. *Journal of Environmental Economics and*
808 *Management*, 91, 150–165. <https://doi.org/10.1016/j.jeem.2018.08.002>

809 Dube, K., Nhamo, G., & Chikodzi, D. (2022). Climate change-induced droughts and tourism:
810 Impacts and responses of Western Cape province, South Africa. *Journal of Outdoor*
811 *Recreation and Tourism*, 39, 100319. <https://doi.org/10.1016/j.jort.2020.100319>

812 Eberhart, R. C., & Shi, Y. (2001). Tracking and optimizing dynamic systems with particle
813 swarms. In *Proceedings of the 2001 Congress on Evolutionary Computation (IEEE Cat.*
814 *No.01TH8546)* (Vol. 1, pp. 94–100 vol. 1). <https://doi.org/10.1109/CEC.2001.934376>

815 Eck, H. V., & Musick, J. T. (1979). Plant Water Stress Effects on Irrigated Grain Sorghum. I.
816 Effects on Yield. *Crop Science*, 19(5), crops1979.0011183X001900050009x.
817 <https://doi.org/10.2135/cropsci1979.0011183X001900050009x>

818 Fang, G. H., Yang, J., Chen, Y. N., & Zammit, C. (2015). Comparing bias correction methods in
819 downscaling meteorological variables for a hydrologic impact study in an arid area in
820 China. *Hydrology and Earth System Sciences*, 19(6), 2547–2559.
821 <https://doi.org/10.5194/hess-19-2547-2015>

822 Fazel, F., Ansari, H., & Aguilar, J. (2023). Determination of the Most Efficient Forage Sorghum
823 Irrigation Scheduling Strategies in the U.S. Central High Plains Using the AquaCrop
824 Model and Field Experiments. *Agronomy*, 13(10), 2446.
825 <https://doi.org/10.3390/agronomy13102446>

826 Feltman, B. (2024). *Sustaining Water Resources and Communities Through Local Collaborative*
827 *Governance* (Ph.D.). Michigan State University, United States -- Michigan. Retrieved
828 from
829 <https://www.proquest.com/docview/3047749156/abstract/897AD25806E74ADFPQ/1>

830 Foster, T., Brozović, N., Butler, A. P., Neale, C. M. U., Raes, D., Steduto, P., et al. (2017).
831 AquaCrop-OS: An open source version of FAO’s crop water productivity model.
832 *Agricultural Water Management*, 181, 18–22.
833 <https://doi.org/10.1016/j.agwat.2016.11.015>

834 GMD 4 LEMA. (2024). Retrieved October 23, 2024, from <https://gmd4.org/LEMA.html>

835 Gorelick, S. M., & Zheng, C. (2015). Global change and the groundwater management
836 challenge. *Water Resources Research*, 51(5), 3031–3051.
837 <https://doi.org/10.1002/2014WR016825>

838 Gupta, H. V., Kling, H., Yilmaz, K. K., & Martinez, G. F. (2009). Decomposition of the mean
839 squared error and NSE performance criteria: Implications for improving hydrological

840 modelling. *Journal of Hydrology*, 377(1), 80–91.
841 <https://doi.org/10.1016/j.jhydrol.2009.08.003>

842 Haacker, E. M. K., Cotterman, K. A., Smidt, S. J., Kendall, A. D., & Hyndman, D. W. (2019).
843 Effects of management areas, drought, and commodity prices on groundwater decline
844 patterns across the High Plains Aquifer. *Agricultural Water Management*, 218, 259–273.
845 <https://doi.org/10.1016/j.agwat.2019.04.002>

846 Heng, L. K., Hsiao, T., Evett, S., Howell, T., & Steduto, P. (2009). Validating the FAO
847 AquaCrop Model for Irrigated and Water Deficient Field Maize. *Agronomy Journal*,
848 101(3), 488–498.

849 Herman, J., & Usher, W. (2017). SALib: An open-source Python library for sensitivity analysis.
850 *Journal of Open Source Software*, 2(9). Doi:10.21105/Joss.00097.

851 High Plains aquifer | U.S. Geological Survey. (2024). Retrieved September 10, 2024, from
852 <https://www.usgs.gov/mission-areas/water-resources/science/high-plains-aquifer>

853 Hu, Y., & Beattie, S. (2019). Role of Heterogeneous Behavioral Factors in an Agent-Based
854 Model of Crop Choice and Groundwater Irrigation. *Journal of Water Resources Planning
855 and Management*, 145(2), 04018100. [https://doi.org/10.1061/\(ASCE\)WR.1943-
856 5452.0001033](https://doi.org/10.1061/(ASCE)WR.1943-5452.0001033)

857 Jaiswal, R., Mall, R. K., Singh, N., Lakshmi Kumar, T. V., & Niyogi, D. (2022). Evaluation of
858 Bias Correction Methods for Regional Climate Models: Downscaled Rainfall Analysis
859 Over Diverse Agroclimatic Zones of India. *Earth and Space Science*, 9(2),
860 e2021EA001981. <https://doi.org/10.1029/2021EA001981>

861 Jones, J. W., Hoogenboom, G., Porter, C. H., Boote, K. J., Batchelor, W. D., Hunt, L. A., et al.
862 (2003). The DSSAT cropping system model. *European Journal of Agronomy*, 18(3),
863 235–265. [https://doi.org/10.1016/S1161-0301\(02\)00107-7](https://doi.org/10.1016/S1161-0301(02)00107-7)

864 Kansas Mesonet · Soil Moisture. (2024). Retrieved September 28, 2024, from [https://mesonet.k-
865 state.edu/agriculture/soilmoist/#tab=chart-tab](https://mesonet.k-state.edu/agriculture/soilmoist/#tab=chart-tab)

866 Kaur, K., & Kaur, N. (2023). Comparison of bias correction methods for climate change
867 projections in the lower Shivaliks of Punjab. *Journal of Water and Climate Change*,
868 14(8), 2606–2625. <https://doi.org/10.2166/wcc.2023.503>

869 Kelly, T. D., & Foster, T. (2021). AquaCrop-OSPy: Bridging the gap between research and
870 practice in crop-water modeling. *Agricultural Water Management*, 254, 106976.
871 <https://doi.org/10.1016/j.agwat.2021.106976>

872 Kennedy, J., & Eberhart, R. (1995). Particle swarm optimization. In *Proceedings of ICNN'95 -
873 International Conference on Neural Networks* (Vol. 4, pp. 1942–1948 vol.4).
874 <https://doi.org/10.1109/ICNN.1995.488968>

875 Kiparsky, M., Milman, A., Owen, D., & Fisher, A. T. (2017). The Importance of Institutional
876 Design for Distributed Local-Level Governance of Groundwater: The Case of
877 California's Sustainable Groundwater Management Act. *Water*, 9(10), 755.
878 <https://doi.org/10.3390/w9100755>

879 Klocke, N., Currie, R., Tomsicek, D., & Koehn, J. W. (2012). Corn Yield Response to Deficit

880 Irrigation. *Transactions of the ASABE*, 55. <https://doi.org/10.13031/2013.41526>

881 Kucharik, C. J. (2003). Evaluation of a Process-Based Agro-Ecosystem Model (Agro-IBIS)
882 across the U.S. Corn Belt: Simulations of the Interannual Variability in Maize Yield.
883 Retrieved from [https://journals.ametsoc.org/view/journals/eint/7/14/1087-](https://journals.ametsoc.org/view/journals/eint/7/14/1087-3562_2003_007_0001_eoapam_2.0.co_2.xml)
884 [3562_2003_007_0001_eoapam_2.0.co_2.xml](https://journals.ametsoc.org/view/journals/eint/7/14/1087-3562_2003_007_0001_eoapam_2.0.co_2.xml)

885 Lamm, F., Rogers, D., Aguilar, J., & Kisekka, I. (2014). Deficit Irrigation of Grain And Oilseed
886 Crops. In *ResearchGate*. Retrieved from
887 [https://www.researchgate.net/publication/268982644_Deficit_Irrigation_of_Grain_And_](https://www.researchgate.net/publication/268982644_Deficit_Irrigation_of_Grain_And_Oilseed_Crops)
888 [Oilseed_Crops](https://www.researchgate.net/publication/268982644_Deficit_Irrigation_of_Grain_And_Oilseed_Crops)

889 Lamsal, A., Welch, S. M., White, J. W., Thorp, K. R., & Bello, N. M. (2018). Estimating
890 parametric phenotypes that determine anthesis date in *Zea mays*: Challenges in
891 combining ecophysiological models with genetics. *PLOS ONE*, 13(4), e0195841.
892 <https://doi.org/10.1371/journal.pone.0195841>

893 Lapides, D. A., Zipper, S., & Hammond, J. C. (2023). Identifying hydrologic signatures
894 associated with streamflow depletion caused by groundwater pumping. *Hydrological*
895 *Processes*, 37(4), e14877. <https://doi.org/10.1002/hyp.14877>

896 Lin, C.-Y., Orduna Alegria, M. E., Dhakal, S., Zipper, S., & Marston, L. (2024). PyCHAMP: A
897 crop-hydrological-agent modeling platform for groundwater management. *Environmental*
898 *Modelling & Software*, 181, 106187. <https://doi.org/10.1016/j.envsoft.2024.106187>

899 Liu, M., He, J., Huang, Y., Tang, T., Hu, J., & Xiao, X. (2022). Algal bloom forecasting with
900 time-frequency analysis: A hybrid deep learning approach. *Water Research*, 219, 118591.
901 <https://doi.org/10.1016/j.watres.2022.118591>

902 Lu, Y., Chibarabada, T. P., McCabe, M. F., De Lannoy, G. J. M., & Sheffield, J. (2021). Global
903 sensitivity analysis of crop yield and transpiration from the FAO-AquaCrop model for
904 dryland environments. *Field Crops Research*, 269, 108182.
905 <https://doi.org/10.1016/j.fcr.2021.108182>

906 Marston, L. T., Zipper, S., Smith, S. M., Allen, J. J., Butler, J. J., Gautam, S., & Yu, D. J. (2022).
907 The importance of fit in groundwater self-governance. *Environmental Research Letters*,
908 17(11), 111001. <https://doi.org/10.1088/1748-9326/ac9a5e>

909 Masasi, B., Taghvaeian, S., Gowda, P. H., Warren, J., & Marek, G. (2019). Simulating Soil
910 Water Content, Evapotranspiration, and Yield of Variably Irrigated Grain Sorghum Using
911 AquaCrop. *JAWRA Journal of the American Water Resources Association*, 55(4), 976–
912 993. <https://doi.org/10.1111/1752-1688.12757>

913 McCown, R. L., Hammer, G. L., Hargreaves, J. N. G., Holzworth, D. P., & Freebairn, D. M.
914 (1996). APSIM: a novel software system for model development, model testing and
915 simulation in agricultural systems research. *Agricultural Systems*, 50(3), 255–271.
916 [https://doi.org/10.1016/0308-521X\(94\)00055-V](https://doi.org/10.1016/0308-521X(94)00055-V)

917 Miller, J. (2018). Corn Reproduction and High Temperatures | Delaware Agronomy Blog.
918 Retrieved October 7, 2024, from [https://sites.udel.edu/agronomy/2018/07/06/corn-](https://sites.udel.edu/agronomy/2018/07/06/corn-reproduction-and-high-temperatures/)
919 [reproduction-and-high-temperatures/](https://sites.udel.edu/agronomy/2018/07/06/corn-reproduction-and-high-temperatures/)

- 920 Miller, M. M., Jones, C. E., Sangha, S. S., & Bekaert, D. P. (2020). Rapid drought-induced land
921 subsidence and its impact on the California aqueduct. *Remote Sensing of Environment*,
922 251, 112063. <https://doi.org/10.1016/j.rse.2020.112063>
- 923 Ndlovu, W. (2024). Assessing the Effectiveness and Resilience of Groundwater Self-
924 Management Practices Using AquaCrop: A Case Study of the Northwestern Kansas
925 Local Enhanced Management Areas. Retrieved March 16, 2025, from
926 <https://www.proquest.com/docview/3160666385>
- 927 Noel, M. M. (2012). A new gradient based particle swarm optimization algorithm for accurate
928 computation of global minimum. *Applied Soft Computing*, 12(1), 353–359.
929 <https://doi.org/10.1016/j.asoc.2011.08.037>
- 930 Northwest Kansas Groundwater Management District No. 4: Revised Management Plan. (2021).
931 GMD4. Retrieved from <https://gmd4.org/Management/GMD4-MgtPro.pdf>
- 932 Nyakudya, I. W., & Stroosnijder, L. (2014). Effect of rooting depth, plant density and planting
933 date on maize (*Zea mays* L.) yield and water use efficiency in semi-arid Zimbabwe:
934 Modelling with AquaCrop. *Agricultural Water Management*, 146, 280–296.
935 <https://doi.org/10.1016/j.agwat.2014.08.024>
- 936 Obembe, O. S., Hendricks, N. P., & Jagadish, S. V. K. (2023). Changes in groundwater irrigation
937 withdrawals due to climate change in Kansas. *Environmental Research Letters*, 18(9),
938 094041. <https://doi.org/10.1088/1748-9326/acf147>
- 939 Onyekwelu, I., Zipper, S., Welch, S., & Sharda, V. (2024, December 24). Quantifying Climate
940 Change Impacts on Maize Productivity Under Different Irrigation Management
941 Strategies: A High-Resolution Spatial Analysis in the U.S. Great Plains. SSRN Scholarly
942 Paper, Rochester, NY: Social Science Research Network.
943 <https://doi.org/10.2139/ssrn.5069870>
- 944 Orduña Alegria, M. E. (2021). Optimization of Agro-Socio-Hydrological Networks under Water
945 Scarcity Conditions.
- 946 Orduña Alegria, M. E., Zipper, S., Shin, H. C., Deines, J. M., Hendricks, N. P., Allen, J. J., et al.
947 (2024). Unlocking aquifer sustainability through irrigator-driven groundwater
948 conservation. *Nature Sustainability*, 7(12), 1574–1583. [https://doi.org/10.1038/s41893-](https://doi.org/10.1038/s41893-024-01437-0)
949 [024-01437-0](https://doi.org/10.1038/s41893-024-01437-0)
- 950 Paredes, P., de Melo-Abreu, J. P., Alves, I., & Pereira, L. S. (2014). Assessing the performance
951 of the FAO AquaCrop model to estimate maize yields and water use under full and
952 deficit irrigation with focus on model parameterization. *Agricultural Water Management*,
953 144, 81–97. <https://doi.org/10.1016/j.agwat.2014.06.002>
- 954 Peters, C. N., Kimsal, C., Frederiks, R. S., Paldor, A., McQuiggan, R., & Michael, H. A. (2022).
955 Groundwater pumping causes salinization of coastal streams due to baseflow depletion:
956 Analytical framework and application to Savannah River, GA. *Journal of Hydrology*,
957 604, 127238. <https://doi.org/10.1016/j.jhydrol.2021.127238>
- 958 Raes, D., Steduto, P., Hsiao, T., & Fereres, E. (2023, August). Reference Manual, Annexes –
959 AquaCrop, Version 7.0.

960 Ran, H., Kang, S., Hu, X., Yao, N., Li, S., Wang, W., et al. (2022). A framework to quantify
961 uncertainty of crop model parameters and its application in arid Northwest China.
962 *Agricultural and Forest Meteorology*, 316, 108844.
963 <https://doi.org/10.1016/j.agrformet.2022.108844>

964 Reilly, J., Tubiello, F., McCarl, B., Abler, D., Darwin, R., Fuglie, K., et al. (2003). U.S.
965 Agriculture and Climate Change: New Results. *Climatic Change*, 57(1), 43–67.
966 <https://doi.org/10.1023/A:1022103315424>

967 Reynolds, C. W. (1987). Flocks, herds and schools: A distributed behavioral model. In
968 *Proceedings of the 14th annual conference on Computer graphics and interactive*
969 *techniques* (pp. 25–34). New York, NY, USA: Association for Computing Machinery.
970 <https://doi.org/10.1145/37401.37406>

971 Saltelli, A., Bamber, G., Bruno, I., Charters, E., Di Fiore, M., Didier, E., et al. (2020). Five ways
972 to ensure that models serve society: a manifesto. *Nature*, 582(7813), 482–484.
973 <https://doi.org/10.1038/d41586-020-01812-9>

974 Sandhu, R., & Irmak, S. (2019). Performance of AquaCrop model in simulating maize growth,
975 yield, and evapotranspiration under rainfed, limited and full irrigation. *Agricultural*
976 *Water Management*, 223, 105687. <https://doi.org/10.1016/j.agwat.2019.105687>

977 Schneider, A. D., & Howell, T. (1998). LEPA and spray irrigation of corn - Southern High
978 Plains. Retrieved from <https://doi.org/10.13031/2013.17313>

979 Steduto, P., Hsiao, T. C., Raes, D., & Fereres, E. (2009). AquaCrop—The FAO Crop Model to
980 Simulate Yield Response to Water: I. Concepts and Underlying Principles. *Agronomy*
981 *Journal*, 101(3), 426–437. <https://doi.org/10.2134/agronj2008.0139s>

982 Teatini, P., Ferronato, M., Gambolati, G., & Gonella, M. (2006). Groundwater pumping and land
983 subsidence in the Emilia-Romagna coastland, Italy: Modeling the past occurrence and the
984 future trend. *Water Resources Research*, 42(1). <https://doi.org/10.1029/2005WR004242>

985 Turner, S. W. D., Hejazi, M., Yonkofski, C., Kim, S. H., & Kyle, P. (2019). Influence of
986 Groundwater Extraction Costs and Resource Depletion Limits on Simulated Global
987 Nonrenewable Water Withdrawals Over the Twenty-First Century. *Earth's Future*, 7(2),
988 123–135. <https://doi.org/10.1029/2018EF001105>

989 Umapathy, P., Venkateshaiah, C., & Arumugam, M. S. (2010). Particle Swarm Optimization
990 with Various Inertia Weight Variants for Optimal Power Flow Solution. *Discrete*
991 *Dynamics in Nature and Society*, 2010, e462145. <https://doi.org/10.1155/2010/462145>

992 USDA - National Agricultural Statistics Service - Charts and Maps - County Maps. (2023).
993 Retrieved October 30, 2023, from
994 https://www.nass.usda.gov/Charts_and_Maps/Crops_County/

995 USDA National Agricultural Statistics Service Cropland Data Layer. (2023). Retrieved October
996 28, 2023, from [https://developers.google.com/earth-](https://developers.google.com/earth-engine/datasets/catalog/USDA_NASS_CD_L)
997 [engine/datasets/catalog/USDA_NASS_CD_L](https://developers.google.com/earth-engine/datasets/catalog/USDA_NASS_CD_L)

998 USDA/NASS QuickStats Ad-hoc Query Tool. (2023). Retrieved September 28, 2024, from
999 <https://quickstats.nass.usda.gov/>

- 1000 Weir, A. H., Bragg, P. L., Porter, J. R., & Rayner, J. H. (1984). A winter wheat crop simulation
1001 model without water or nutrient limitations. *The Journal of Agricultural Science*, *102*(2),
1002 371–382. <https://doi.org/10.1017/S0021859600042702>
- 1003 Whittemore, D. O., Butler, J. J., & Wilson, B. B. (2023). 2023 Status of the High Plains Aquifer
1004 in Kansas.
- 1005 Whittemore, D. O., Butler, J. J., Bohling, G. C., & Wilson, B. B. (2023). Are we saving water?
1006 Simple methods for assessing the effectiveness of groundwater conservation measures.
1007 *Agricultural Water Management*, *287*, 108408.
1008 <https://doi.org/10.1016/j.agwat.2023.108408>
- 1009 WIMAS. (2023). Retrieved October 30, 2023, from
1010 https://geohydro.kgs.ku.edu/geohydro/wimas/query_setup.cfm
- 1011 Xing, H., Xu, X., Li, Z., Chen, Y., Feng, H., Yang, G., & Chen, Z. (2017). Global sensitivity
1012 analysis of the AquaCrop model for winter wheat under different water treatments based
1013 on the extended Fourier amplitude sensitivity test. *Journal of Integrative Agriculture*,
1014 *16*(11), 2444–2458. [https://doi.org/10.1016/S2095-3119\(16\)61626-X](https://doi.org/10.1016/S2095-3119(16)61626-X)
- 1015 Zelelew, M. B., & Alfredsen, K. (2013). Sensitivity-guided evaluation of the HBV hydrological
1016 model parameterization. *Journal of Hydroinformatics*, *15*(3), 967–990.
1017 <https://doi.org/10.2166/hydro.2012.011>
- 1018 Zhao, K., Tao, Y., Liu, M., Yang, D., Zhu, M., Ding, J., et al. (2022). Does temporary heat stress
1019 or low temperature stress similarly affect yield, starch, and protein of winter wheat grain
1020 during grain filling? *Journal of Cereal Science*, *103*, 103408.
1021 <https://doi.org/10.1016/j.jcs.2021.103408>
- 1022 Zipper, S., Kastens, J., Foster, T., Wilson, B. B., Melton, F., Grinstead, A., et al. (2024).
1023 Estimating irrigation water use from remotely sensed evapotranspiration data: Accuracy
1024 and uncertainties at field, water right, and regional scales. *Agricultural Water*
1025 *Management*, *303*, 109036. <https://doi.org/10.1016/j.agwat.2024.109036>
- 1026 Zipper, S., Brookfield, A., Ajami, H., Ayers, J. R., Beightel, C., Fienen, M. N., et al. (2024).
1027 Streamflow Depletion Caused by Groundwater Pumping: Fundamental Research
1028 Priorities for Management-Relevant Science. *Water Resources Research*, *60*(5),
1029 e2023WR035727. <https://doi.org/10.1029/2023WR035727>
- 1030 Zipper, S., Ifft, J., Orduña Alegría, M. E., Butler, J. J., Marston, L. T., Yu, Q., & Metzger, S.
1031 (2024). *Water management challenges and potential solutions related to the U.S. federal*
1032 *crop insurance program* (KGS Open-File Report 2024-11 No. 2024–11) (p. 20).
1033 Lawrence KS: Kansas Geological Survey. Retrieved from
1034 <https://www.kgs.ku.edu/Publications/OFR/2024/OFR2024-11.pdf>
- 1035 Zwickle, A., Feltman, B., Brady, A., Kendall, A., & Hyndman, D. (2021). Sustainable irrigation
1036 through local collaborative governance: Evidence for a structural fix in Kansas.
1037 *Environmental Science & Policy*, *124*, 517–526.
1038 <https://doi.org/10.1016/j.envsci.2021.07.021>
- 1039

1040 **Supplementary material**

1041 ***AquaCrop Irrigation Calculation***

1042 The irrigation depth (*Irrig Depth*) is calculated daily as follows: the root zone depletion
1043 stress indicator is first calculated as the proportion of the soil water depletion (amount of
1044 available water that is required to bring to water amount back to FC) and total available water
1045 (*TAW*). This stress indicator varies from zero (full stress) to one (no stress). Whenever the root
1046 zone depletion is greater than smt_{gs} , the user specified soil moisture threshold for irrigation in
1047 each of the four crop growth stages, an irrigation requirement (*Irrig Req*) equal to the soil water
1048 depletion is calculated as shown in **Eq. S2**. To account for irrigation efficiency, the irrigation
1049 requirement is multiplied by an application efficiency adjustment (*Ieff*), which is expressed as a
1050 percentage with higher values indicating greater efficiency (the current model runs with an
1051 efficiency adjustment of 85%). The *Irrig Depth* is then calculated as the minimum between the
1052 *Irrig Req* and the specified maximum irrigation depth (*Irrig_{max}*) per event (the model default
1053 value for *Irrig_{max}* is 25 mm) using **Eq S3**.

1054

$$1055 \text{Root Zone Depletion } (Dr) > 1 - smt_{gs}/100 \quad (S1)$$

$$1056 \text{Irrig Req} = \max(0, \text{soil water depletion}) \quad (S2)$$

$$1057 \text{Irrig Depth} = \min(\text{Irrig}_{max}, \text{Irrig Req} * Ieff) \quad (S3)$$

1058 ***Sensitivity Analysis using Sobol Method***

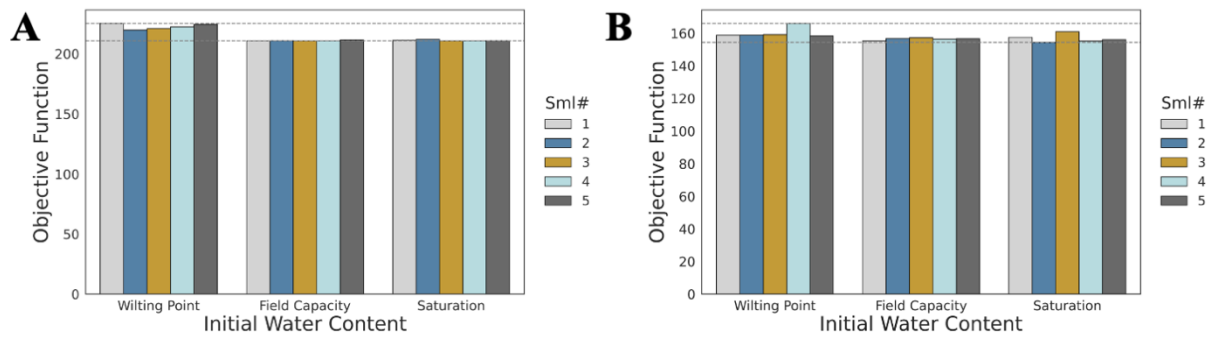
1059 The Sobol method (Sobol, 1990) was applied to crop parameters related to (1) crop
1060 development and transpiration, (2) biomass and yield, (4) water stress, and (4) management
1061 using the *SALib* Python package (Herman & Usher, 2017). We adjusted the maximum irrigation,
1062 water stress and temperature stress parameters as shown in Table S2, and the remaining
1063 parameters were set to the model defaults for that crop. The maximum daily and seasonal
1064 irrigation depths for both crops were estimated based on field studies done by Kansas State
1065 Research and Extension scientists (Ciampitti et al., 2022, 2023).

1066 We analyzed the first, second and total indices using the Sobol function from the *SALib*
1067 Python package (Herman & Usher, 2017). For both the yield and water use simulations, 2^N and
1068 2^{15} samples were generated from the parameter space where n is a series of one-unit increments
1069 from one to ten to ensure model convergence and stability. This sampling scheme creates a total
1070 of $n(2k+2)$ model runs where n and k are the number of samples and parameters, respectively.
1071 We applied this approach to all the scenarios (for example, irrigated corn and sorghum under
1072 dry, normal, and wet conditions) using yield and irrigation water use as individual target outputs
1073 for both crops of interest. Due to the large computational needs, we used the Blanca distributed
1074 High-Performance-Computing (HPC) system (<https://www.colorado.edu/rc/resources/blanca>).
1075 To distinguish between the influential and non-influential parameters, we defined a threshold:

1076 parameters with total order indices (ST) greater than 10% of the maximum ST from each
1077 scenario were defined as influential.

1078 ***Influence of initial soil moisture conditions on performance***

1079 Varying the initial soil water conditions (*field capacity (FC)*, *saturation (SAT)* or *wilting point*
1080 (*WP*)) for corn and sorghum did not have a major influence on model fit (Fig. S1). The objective
1081 function results were nearly identical for *FC* and *SAT* models, while the *WP* models had higher
1082 objective function values (indicating a worse agreement with observations) and more variation
1083 within the group. For our analysis, we determined that models calibrated under *FC* conditions
1084 produced the lowest objective functions (Fig. S1) and represented the typical soil water content
1085 ranges in the GMD-4 region (“Kansas Mesonet · Soil Moisture,” 2024).
1086

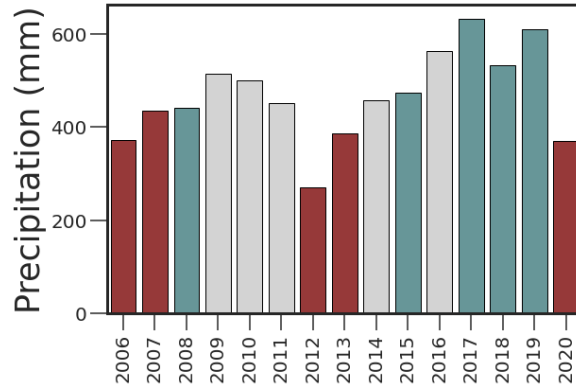


1087

1088 **Figure S1.** Objective function values for corn (A) and sorghum (B) models from the Particle
1089 Swarm Optimization (PSO) calibrations performed using 80% of the observed yield and
1090 irrigation depth data. For each initial water content, Sml#1-5 correspond to different random
1091 model input realizations (see Section 3.3.2).

1092

1093



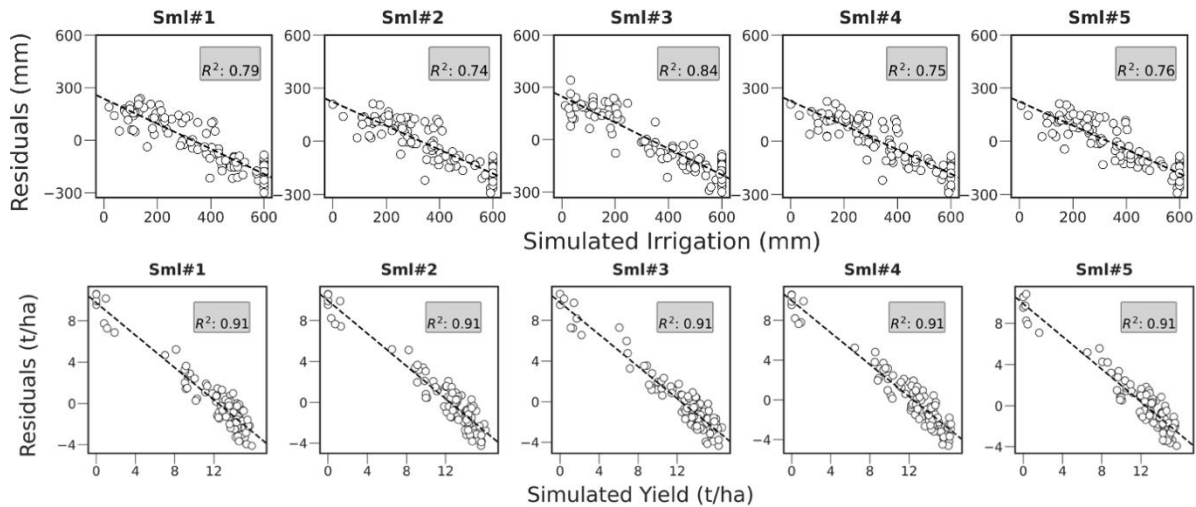
1094

1095 **Figure S2.** Average irrigation season (Jan – Sept) precipitation in the GMD-4 region. Red bars
 1096 represent the five driest years over the 2006 - 2020 period. Blue bars represent five randomly
 1097 selected non-drought years for the model spin up period.

1098

1099

1100

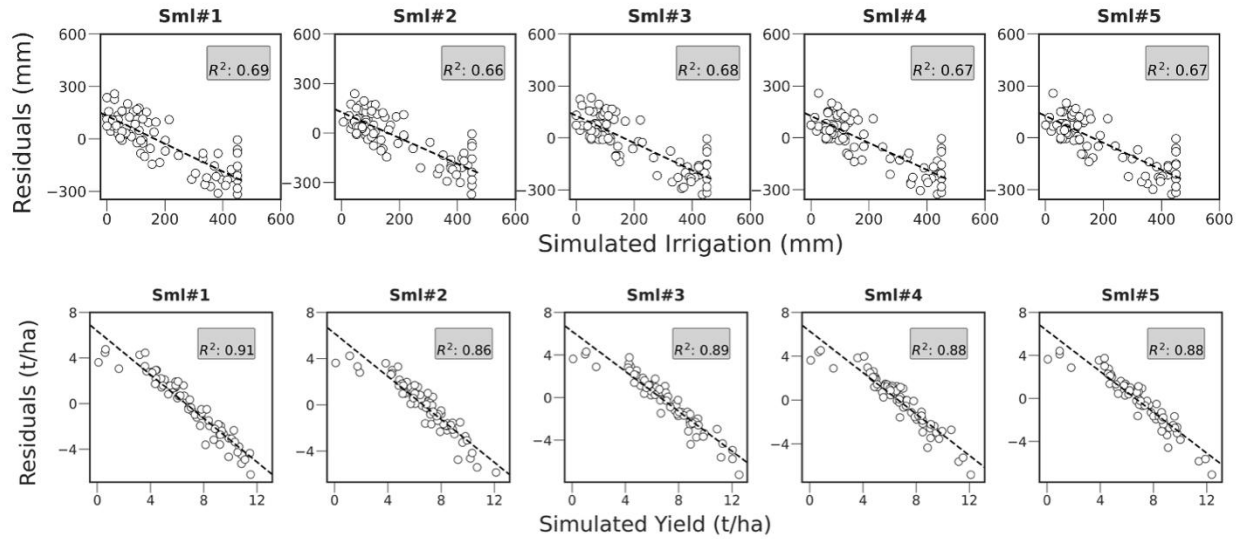


1101

1102 **Figure S3.** Corn residuals for yield and irrigation as a function of simulated yield and irrigation.
 1103 These relationships are used for modified-difference bias correction. These results all use field
 1104 capacity as the initial soil moisture condition, and Sml#1-5 correspond to different random
 1105 model input realizations (see Section 3.3.2). Sml#2 was selected as the best corn model and used
 1106 for results shown in the main text. Fit statistics are in Table S3.

1107

1108



1109

1110 **Figure S4.** Sorghum residuals for yield and irrigation as a function of simulated yield and
 1111 irrigation. These relationships are used for modified-difference bias correction. These results all
 1112 use field capacity as the initial soil moisture condition, and Sml#1-5 correspond to different
 1113 random model input realizations (see Section 3.3.2). Sml#2 was selected as the best sorghum
 1114 model and used for results shown in the main text. Fit statistics are in Table S4.

1115

1116 **Table S1.** Model parameters used for the sensitivity analysis of corn and sorghum. Highlighted
 1117 rows indicate parameters considered only for corn and the remaining parameters were used for
 1118 both crops.

Parameter	Description	Units	Lower Bound	Upper Bound
<u>Crop Development and Transpiration</u>				
ccx	maximum fractional canopy cover size	-	0.85	0.99
rtx	maximum effective rooting depth	m	1.2	2
rtexup	maximum water extraction at the top of the root zone	m ³ /m ³ /day	0.02	0.03
rtexlw	maximum water extraction at the bottom of the root zone	m ³ /m ³ /day	0	0.01
kc	crop coefficient when canopy is complete but prior to senescence	-	1.0	1.1
<u>Biomass and Yield</u>				
wp	water productivity normalized for reference ET0 and CO2	g/m ²	30	35
hi	reference harvest index	-	0.45	0.55
<u>Water Stress</u>				
hipsveg	coefficient describing positive impact of restricted vegetative growth during yield formation on HI	-	0.5	10.0
hingsto	coefficient describing negative impact of stomatal closure growth during yield formation on HI	-	1.0	20.0
<u>Irrigation Management</u>				
smt1	soil moisture threshold during crop emergence and canopy growth	%	40	80
smt2	soil moisture threshold during crop maximum canopy	%	0	50
smt3	soil moisture threshold during crop canopy senescence	%	0	50

1119

1120

1121 **Table S2.** Default parameter values used for the corn and sorghum sensitivity analysis.

Parameter	Description	Corn Default Value	Sorghum Default Value
max_irr	maximum depth (mm) that can be applied each day	6.5	6.5
max_irr_season	maximum depth (mm) that can be applied each season	600	450
p_up2	upper soil water depletion threshold for water stress effects on canopy stomatal control	0.45	0.55
p_up3	upper soil water depletion threshold for water stress effects on canopy senescence	0.6	0.85
cdc	canopy decline coefficient (fraction per GDD/calendar day)	1.31	-
tmax_lo	maximum air temperature (degC) at which pollination completely fails	33	-
tmax_up	maximum air temperature (degC) above which pollination begins to fail	38	-

1122

1123

1124 **Table S3.** Model performance evaluation for corn irrigation depth (mm) and yield (t/ha). Red
 1125 shading indicates the bias-corrected model with the best fit metrics and blue shading indicates
 1126 the best model based on the calibration, validation and bias-correction results. For irrigation,
 1127 Sml#1 and Sml#2 had the best fit metrics after bias correction.

CORN IRRIGATION (mm)				
Model	Evaluation Metric	KGE	RMSE	NRMSE
Sml#1	Calibration	-0.22	145	0.43
	Validation	-0.20	157	0.43
	Bias-Corrected Validation	0.41	79	0.22
Sml#2	Calibration	-0.01	127	0.38
	Validation	0.04	138	0.38
	Bias-Corrected Validation	0.41	79	0.22
Sml#3	Calibration	-0.46	164	0.49
	Validation	-0.24	166	0.45
	Bias-Corrected Validation	0.30	83	0.23
Sml#4	Calibration	-0.06	131	0.39
	Validation	0.05	139	0.38
	Bias-Corrected Validation	0.36	81	0.22
Sml#5	Calibration	-0.06	129	0.39
	Validation	-0.01	142	0.39
	Bias-Corrected Validation	0.41	80	0.22
CORN YIELD (t/ha)				
Model	Evaluation Metric	KGE	RMSE	NRSME
Sml#1	Calibration	-1.00	3.2	0.26
	Validation	-0.64	3.4	0.27
	Bias-Corrected Validation	0.44	1.2	0.10
Sml#2	Calibration	-1.10	3.3	0.27
	Validation	-0.73	3.5	0.28
	Bias-Corrected Validation	0.44	1.2	0.10
Sml#3	Calibration	-1.10	3.3	0.26
	Validation	-0.71	3.5	0.28
	Bias-Corrected Validation	0.45	1.2	0.10
Sml#4	Calibration	-1.20	3.4	0.27
	Validation	-0.75	3.5	0.28
	Bias-Corrected Validation	0.43	1.2	0.10
Sml#5	Calibration	-1.10	3.3	0.27
	Validation	-0.67	3.4	0.28
	Bias-Corrected Validation	0.43	1.2	0.10

1128

1129 **Table S4.** Model performance evaluation for sorghum irrigation depth (mm) and yield (t/ha).
 1130 Red shading indicates the bias-corrected model with the best fit metric and blue shading
 1131 indicates the best model based on the calibration, validation and bias-correction results.

SORGHUM IRRIGATION (mm)				
Model	Evaluation Metric	KGE	RMSE	NRSME
Sml#1	Calibration	0.00	149	0.89
	Validation	-0.01	138	0.65
	Bias-Corrected Validation	0.17	85	0.40
Sml#2	Calibration	0.07	143	0.85
	Validation	0.06	133	0.62
	Bias-Corrected Validation	0.14	87	0.41
Sml#3	Calibration	0.03	147	0.87
	Validation	0.00	137	0.64
	Bias-Corrected Validation	0.16	86	0.40
Sml#4	Calibration	0.06	144	0.86
	Validation	-0.02	139	0.65
	Bias-Corrected Validation	0.15	87	0.41
Sml#5	Calibration	0.06	143	0.85
	Validation	0.00	138	0.65
	Bias-Corrected Validation	0.15	87	0.41
SORGHUM YIELD (t/ha)				
Model	Evaluation Metric	KGE	RMSE	NRSME
Sml#1	Calibration	-1.40	2.7	0.41
	Validation	-0.97	2.9	0.41
	Bias-Corrected Validation	-0.17	1.0	0.15
Sml#2	Calibration	-0.81	2.2	0.33
	Validation	-0.69	2.5	0.37
	Bias-Corrected Validation	-0.12	1.0	0.15
Sml#3	Calibration	-1.20	2.5	0.38
	Validation	-1.10	2.9	0.42
	Bias-Corrected Validation	-0.09	1.0	0.15
Sml#4	Calibration	-0.96	2.4	0.35
	Validation	-0.66	2.6	0.37
	Bias-Corrected Validation	-0.14	1.0	0.15
Sml#5	Calibration	-1.00	2.4	0.36
	Validation	-0.82	2.7	0.39
	Bias-Corrected Validation	-0.16	1.0	0.15

1132
 1133